



Autosub Long Range 1500: A continuous 2000 km field trial

Alexander B. Phillips*, Robert Templeton, Daniel Roper, Richard Morrison, Miles Pebody, Philip M. Bagley, Rachel Marlow, Ed Chaney, James Burris, Alberto Consensi, Davide Fenucci, Francesco Fanelli, Achille Martin, Georgios Salavasidis, Owain Jones, Ashley Morris, Catherine A. Harris, Alvaro Lorenzo, Maaten Furlong

Marine Autonomous and Robotic Systems, National Oceanography Centre, European Way, Southampton, SO14 3ZH, United Kingdom

ARTICLE INFO

Keywords:

Autonomous Underwater Vehicles
Field robotics
Control system design
Over-the-horizon operations

ABSTRACT

Long Range Autonomous Underwater Vehicles (LRAUVs) offer the potential to monitor the ocean at higher spatial and temporal resolutions compared to conventional ship-based techniques. The multi-week to multi-month endurance of LRAUVs enables them to operate independently of a support vessel, creating novel opportunities for ocean observation. The National Oceanography Centre's Autosub Long Range is one of a small number of vehicles designed for a multi-month endurance. The latest iteration, Autosub Long Range 1500 (ALR1500), is a 1500 m depth-rated LRAUV developed for ocean science in coastal and shelf seas or in the epipelagic and meteorologic regions of the ocean. This paper presents the design of the ALR1500 and results from a five week continuous deployment from Plymouth, UK, to the continental shelf break and back again, a distance of approximately 2000km which consumed half of the installed energy. The LRAUV was unaccompanied throughout the mission and operated continuously beyond visual line of sight.

1. Introduction

For many applications, Autonomous Underwater Vehicles (AUVs) offer the potential to monitor the global ocean at a much higher temporal and/or spatial resolutions than is possible using conventional ship-based methods. For example, Autonomous Lagrangian floats (e.g. Argo) have demonstrated the power of a distributed network of instruments to enhance our understanding of ocean circulation (Riser et al., 2016); underwater gliders are becoming embedded in the Global Ocean Observing System (GOOS), providing insights into ocean physics, chemistry and biology (Testor et al., 2019); and work class Autonomous Underwater Vehicles (AUVs) are providing unprecedented understanding of the seafloor (Wynn et al., 2014).

The spectrum of AUVs is typically subdivided into classes by size, payload, depth rating and range/endurance. It is within this design space that AUV developers tend to specialise their platforms. Fig. 1 illustrates the mass versus range of some notable AUV platforms illustrating the breadth of specifications available. Implicit (but not shown in Fig. 1) is the variation in payload capacity (power, sensor range, resolution) which tends to increase with the mass axis and reduce with increasing vehicle range. As the core capabilities (i.e. person-portable or work-class vehicles) have become well-established, there has been increasing effort in the development of vehicle types which push at the extremes of these axes. At the smallest size, Micro AUV technologies

are becoming more prevalent, with numerous systems becoming commercially available e.g. Phillips et al. (2017b), Underwood and Murphy (2017) and Manley and Smith (2017). At the largest scale, eXtra Large Uncrewed Undersea Vehicles (XLUUV) are being explored primarily for national security applications (O'Rourke, 2019). However, the cost of XLUUVs is currently prohibitive for oceanographic science applications. Lower cost platforms, such as Underwater gliders (Rudnick et al., 2004), continue to extend the range envelope of AUVs. Also pushing the range axis are Long Range AUVs (LRAUVs) which, unlike underwater gliders, are propeller driven. Thus, LRAUVs combine the mobility and variable speed typical of conventional AUVs with low-power sensor payloads and energy management to extend their range/endurance in a similar manner to gliders.

1.1. Long range AUVs

Tethys (Bellingham et al., 2010; Hobson et al., 2012) is one of the most established LRAUV platforms, developed by the Monterey Bay Aquarium Research Institute (MBARI). Tethys is a relatively small person-portable 120 kg AUV (0.3 m diameter and 2 m length) with a 300 m depth rating. With a multi-week endurance (depending on payload and speed — range 0.5 to 1 m/s), Tethys vehicles have been

* Corresponding author.

E-mail address: abp@noc.ac.uk (A.B. Phillips).

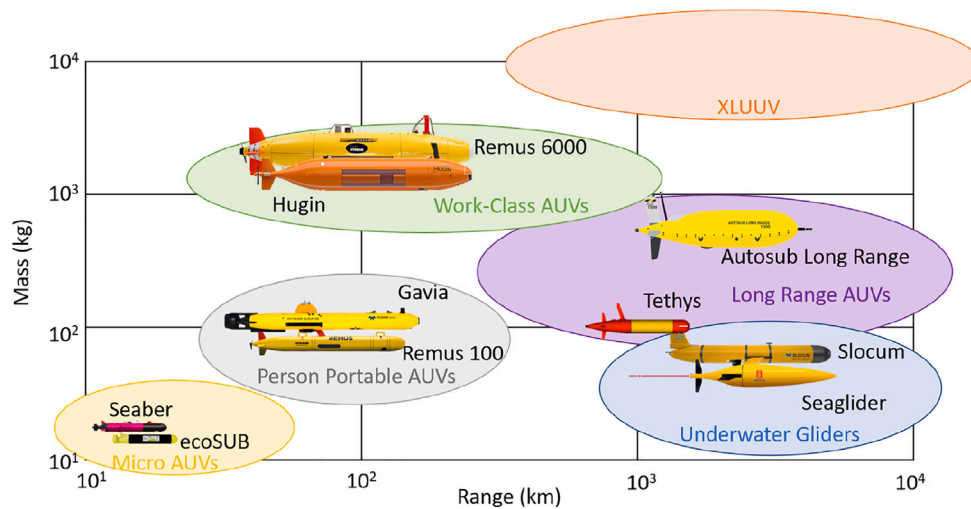


Fig. 1. Range and mass for different classes of AUVs (values indicative).
Source: adapted from Duguid and Camilli (2021).

utilised for a range of applications including monitoring phytoplankton blooms (Godin et al., 2011), upwelling fronts (Zhang et al., 2012) and oil spills in Arctic environments (Kukulya et al., 2016).

Autosub Long Range 6000 (ALR6000) (Roper et al., 2021) is a 6000 m depth-rated autonomous underwater vehicle capable of operating for two to three months in a single deployment, with a range of up to 1800 km. This range is an order of magnitude greater than work-class AUVs, e.g. the existing high-powered Autosub6000 vehicle has a range of 180 km and an endurance of 36 h (McPhail, 2009). The long endurance of ALR6000 is achieved through the use of high energy-density lithium primary cells combined with optimisation of energy consumption within all on-board systems. In particular, the increasing availability of low-power sensors developed for the glider community (Hayes et al., 2007) has furnished ALR6000 with a variety of efficient payload options. Science deployments have included ALR6000 successfully conducting multi-day operations in the Southern Ocean (Garabato et al., 2017, 2019; Salavasidis et al., 2019) and under the Ronne-Filchner Ice Shelf (McPhail et al., 2019).

Sea-Whale 2000 is a 3 m long, 2000 m depth-rated hybrid AUV with a nominal range of 1500 km at 0.5 m/s supporting a low-power payload of up to 7 W, including a CTD and ADCP (Huang et al., 2019a). A buoyancy engine and internal moving mass enables the vehicle to undertake a glider-like sawtooth profile or operate like a conventional AUV using the propeller and control planes. The inclusion of a buoyancy engine enables the Sea-Whale to minimise its net buoyancy at any depth reducing the power required to maintain depth (Huang et al., 2019b). Sea-Whale 2000 has demonstrated week-long deployments operating in two modes, profiling and constant depth (Qiu et al., 2020).

This paper describes the design and long distance trial of a new class of LRAUV, Autosub Long Range 1500 (ALR1500), designed to make routine over-the-horizon operations, presenting practical progress against the technical challenges described in Section 2. The remainder of this paper is organised as follows: Section 3 gives an overview of the ALR1500 platform, Sections 4 to 6 provide details of the electro-mechanical design, on-board control system and piloting tool-chain, Section 7 presents results from the vehicles first long-range operations from Plymouth UK, and Section 8 presents conclusions and discusses the potential applications of vehicles with this capability.

2. Challenges

Increasing the range of AUVs from hundreds to thousands of kilometres opens a selection of new applications for AUV technologies.

In particular, the ability to launch AUVs from shore to transit unattended to a work area becomes a viable survey approach, removing the need for a support vessel with its associated financial and carbon implications. However, the transition from conventional short missions to over-the-horizon operation presents a series of technical challenges.

2.1. Persistent underwater autonomy

A key obstacle to long-term missions is the significant uncertainty of an ever-changing environment. When considering longer duration missions, AUVs need to deal with high variability across large-scale spatio-temporal dimensions while reacting to a locally dynamic and uncertain environment. For example, Zhang et al. (2022) implemented an onboard front-following algorithm to enable a Tethys-Class LRAUV to autonomously track salinity-intrusion fronts over shelf for five days. This approach effectively revealed the spatial structure and movement of the front, resulting in the collection of measurements that would of been impossible to achieve with a predefined, pre-planned, trajectory.

2.2. Energy balance

The design of an AUV inevitably leads to compromise on one or more of the key design constraints: size, payload, depth-rating and range/endurance. The original design for ALR6000 (Furlong et al., 2012) targeted a specification of 6000 m depth rating, 6000 km range and 6 months endurance at slow speeds with a low power payload. However, due to practical implementation constraints, the operational vehicle has a significantly compromised range and endurance, due to increased hotel load (vehicle and science payload), lower than predicted propulsive efficiency and lower available installed energy than originally envisaged.

A useful metric for understanding energetic cost is the vehicles Cost of Transport, COT , which equates to the energy cost to transport a unit mass a unit distance ($J kg^{-1} m^{-1}$) (Phillips et al., 2012, 2017a).

$$COT = \frac{P_{tot}}{mU} \quad (1)$$

$$R = \frac{E}{mCOT} \quad (2)$$

$$E = \frac{E}{mCOTU} \quad (3)$$

where P_{tot} is the total time averaged power expended by the system, m is vehicle flooded displacement (kg), U is forward speed, R is vehicle range, E is the onboard energy of the AUV.

The power consumption, P_{tot} , of an AUV can be defined as:

$$P_{tot} = P_H + P_P + P_B, \quad (4)$$

where P_H is the hotel load associated with all systems not directly related to propulsion including consumption due to sensor payloads, communication systems, navigation systems, etc. While hotel load is invariant to forward speed, and propulsion power, P_P , is related to propulsion speed cubed. For a positively or negatively buoyant vehicle trying to maintain a constant depth, additional power is required to overcome the net buoyancy, P_B .

Thus, when considering the range of AUVs, work-class AUVs typically have high COT largely driven by their comparative high speed and high hotel load. Consequently, their range/endurance is limited to hours or days. At the other end of the spectrum, underwater gliders are low power (both propulsion and hotel load) and as such have a low COT and are able to operate for weeks or months (Rudnick et al., 2004). LRAUVs sit between these two groups, minimising their COT by operating at lower speeds than conventional work-class AUVs whilst ensuring low hotel load. The ability of an LRAUV to overcome currents, maintain a constant depth or a fixed altitude above the seabed / below the ice offers a range of complementary capabilities to drifting floats and underwater gliders.

2.3. Underwater navigation

Underwater navigation presents an ongoing challenge for all classes of AUV (Paull et al., 2013) as there is no single robust solution for this complex GPS-denied environment. The default approach is to couple inertial sensors to a Doppler Velocity Log (DVL) and perform simple dead reckoning. Whilst in close proximity to the seabed, this approach can provide good performance (navigation error < 1% distance travelled in a straight line), albeit with unbounded growth in position error. The speed and direction of the AUV can be greatly impacted by movement of the water mass (currents). When operating in mid-water, such movements are unobserved, so high errors can be rapidly generated. For LRAUVs, dead reckoning in isolation may be problematic: firstly, to meet the energy constraints described above, LRAUVs tend to opt for low-power inertial sensors reducing the accuracy of any dead reckoned solution; secondly, the nature of long-range operations means that mission duration can be long and thus the absolute error at the end of the mission may be unacceptably large; and thirdly, many of the applications of LRAUVs require operation mid-water (e.g. studies in the twilight zone) so the convection of the water mass is an important source of error.

A range of approaches have been demonstrated for different AUV types and applications to address these issues, but no universally applicable bounded navigation solution exists for all use cases. Acoustically coupled LRAUVs with long range uncrewed surface vessels (USVs) (Jakuba et al., 2018; Phillips et al., 2018) enables both external position aiding and real-time communications. Terrain-aided navigation (TAN) is a self-contained state estimation technique that can limit the inertial navigation error by statistically matching bathymetric observations to a given bathymetric reference map. This navigation technique is particularly appealing for LRAUVs requiring a simple and effective on-board navigation solution without reliance on external support systems. TAN has been demonstrated for underwater gliders undertaking long range missions in Claus and Bachmayer (2015). The potential of TAN for LRAUVs is presented in Salavasidis et al. (2019) for near-bottom, deep water operation; and Salavasidis et al. (2020) for mid water-column operation. For dives in deep water down to the seabed, where convection in currents can produce large navigation errors before reaching DVL bottom lock, approaches have been proposed that exploit the fact that current profiles of water columns are stable over time. By re-observing the vertical current structure using an Acoustic Doppler Current Profiler (ADCP) during vehicle descent, a history of the current profile can be generated enabling current speeds during the descent to be estimated, e.g. Medagoda et al. (2016) and Feng et al. (2020).

2.4. Communications

Transfer of data or information between the remote operator (human or machine) presents a double challenge for unaccompanied LRAUV operations. Firstly, whilst underwater there is currently no viable technology to enable the LRAUV to transmit data to shore (or vice versa) without resorting to additional fixed or mobile infrastructure (e.g. USV). Secondly, whilst on the surface, communication is limited to the available satellite communication bandwidth with its associated cost and latency. In practice, this limits the volume and timeliness of any data transmissions. As a result, data are then significantly down-sampled or compressed before transmission, limiting operator visibility and ability to reason about piloting decisions.

2.5. Reliability

AUVs are complex mechatronic systems in which a failure of any component can readily lead to: degradation of mission performance, costly interventions such as early recovery of the vehicle or ultimately vehicle loss (Chen et al., 2021). Long term operation over-the-horizon not only increases the duration of missions and thus the likelihood of a failure occurring, but also generates new potential failure modes. For example, when considering multi-week or longer deployments, biofouling becomes a potential cause of failure. Experience with underwater gliders and uncrewed surface vehicles has demonstrated that biofouling can rapidly impact the hydrodynamic performance of the vehicles (Haldeman et al., 2016). Furthermore, for conventional AUVs the focus when considering risk is often on total loss of the system (Brito and Griffiths, 2016) operating in a consistent environment, yet when operating unaccompanied far offshore the need to recover a malfunctioning vehicle can cause an expensive logistical challenge, and the dynamic and changing nature of the environment also needs to be considered (Yang et al., 2020).

2.6. Regulation

Under the guidance and leadership of the International Maritime Organisation (IMO), many countries and institutions in the world have gradually developed industry guidelines and codes for the operation of Marine Autonomous Surface Ships (MASS) (Zhang et al., 2021; Veal, 2020). Among them, the United Kingdom has been developing MASS UK Industry Conduct Principles and Code of Practice (MASRWG, 2021), however when it comes to AUV operations the regulator position is still evolving (Veal et al., 2019).

3. Autosub long range 1500 (ALR1500)

The Autosub programme has been developing AUVs for science applications since the 1980s, for a more complete history see Griffiths (2012). Key achievements include: Autosub 3 successfully exploring under the Pine Island Glacier in 2009 (McPhail et al., 2009) providing unprecedented multi-beam imagery of the underside of the ice (Jenkins et al., 2010; Graham et al., 2013) and Autosub6000 (McPhail, 2009) locating the deepest known hydrothermal vent at nearly 5000 m in the Mid-Cayman Rise (Connelly et al., 2012). More recently, the team's development activities have focused on long-range vehicles, including the ALR6000 vehicles described in Section 1.1.

The Autosub Long Range 1500 (ALR1500) class of vehicles is a substantial evolution of the NOCs existing ALR6000 AUVs. The ability to withstand the hydrostatic pressure at 6000 m comes with a significant volume and weight penalty when operating in shallow water. For many work areas, such as on the UK continental shelf or when operation near ice, a depth-rating of 1500 m is more than sufficient. By designing for a shallower depth-rating, it is possible to develop a vehicle able to carry a larger battery pack and/or additional scientific payload, within the same physical envelope as the original vehicle. As

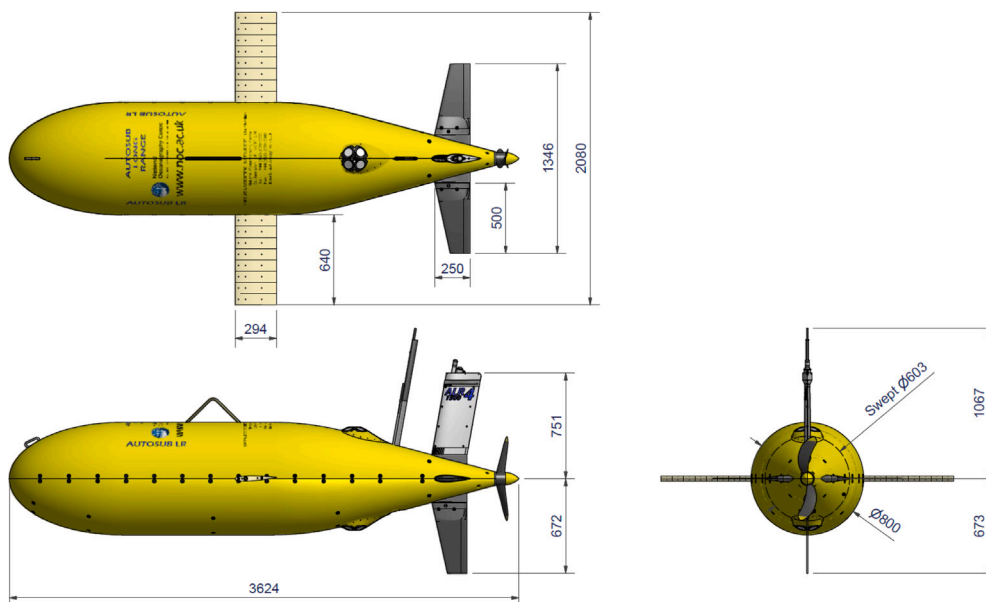


Fig. 2. Autosub Long Range principle dimensions. Note: all dimensions in mm.

Table 1
Autosub long range 1500 — key specifications.

Parameter	Value
Length	3.6 m
Diameter	0.8 m
Dry mass	750 kg
Enclosed displacement	1.3 m ³
Depth rating	1500 m
Cruise speed	0.45 to 0.9 m/s
Standard sensors	CTD (SBE 52-MP) up 500 kHz Nortek ADCP/DVL down 500 kHz Nortek ADCP/DVL
Communications	Iridium Short Burst Data Wifi (2.5 GHz)
Surface buoyancy	25N
On-board energy	max 95 kWh Lithium Thionyl Chloride



Fig. 3. Autosub Long Range 1500 (ALR1500) front and Autosub Long Range 6000 (ALR6000) behind. NOC currently operate three ALR6000 vehicles and three ALR1500 vehicles.

a result, ALR1500 has been designed for an aspiration of six months operation (Roper et al., 2017), covering a range of up to 6000 km in a low power configuration. A specification of the ALR1500 is provided in Table 1 and principle dimensions are illustrated in Fig. 2.

As a platform for science applications, the payload sensor fit is highly variable with the associated implications for ultimate range and endurance. Fig. 4(a) illustrates indicative ALR propulsion power versus speed, data taken from commissioning trials of ALR-2 in Portland Harbour in 2015. Assuming a volumetric drag coefficient of 0.05 these provide total propulsion system efficiency of approximately 40%. Combining this propulsion power with indicative hotel loads provides the range and endurance estimates shown in Fig. 4(b).

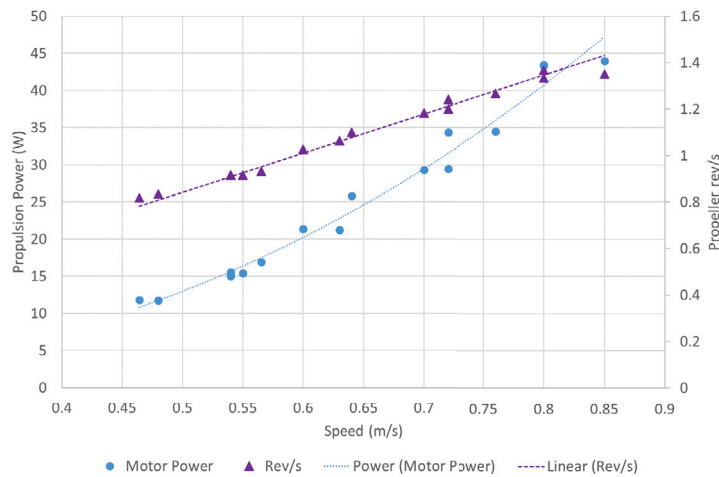
As can be seen in Fig. 3, ALR1500 shares many subsystems with its sister class ALR6000. The most significant change between the classes is the pressure vessel. However during development of the ALR1500 class, upgrades were made to common systems across both classes including: new actuators for the control surfaces, a new on-board control system, a low power navigation system including Terrain Aided Navigation (TAN) and a new web based piloting tool-chain for over-the-horizon operations.

4. Electro-mechanical design

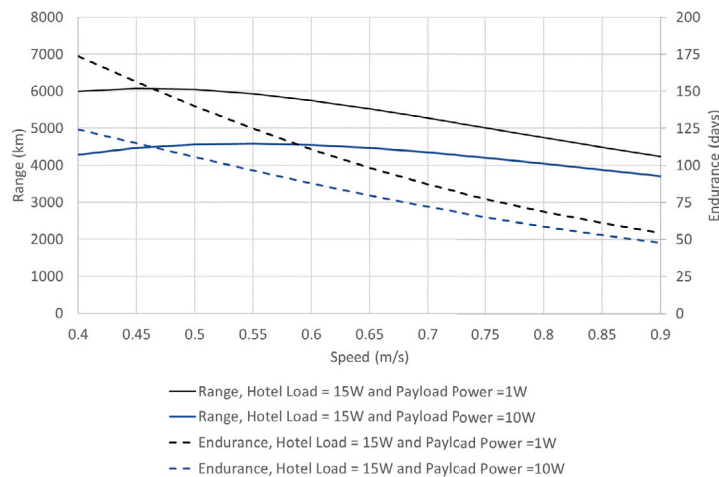
The core of the ALR1500 vehicle is a dome-ended pressure vessel. This comprises of a single ring-stiffened 700 mm diameter by 1000 mm length cylindrical centre section constructed from forged aluminium alloy 7075-T6, and two 700 mm diameter hemispherical end caps cast and machined from Aluminium EN AC42100. The pressure vessel is mounted in a polypropylene boat frame which is covered with a glass reinforced plastic shell to give a hydrodynamic shape enclosing 1.3 m³. Within this structure is approximately 0.4 m³ of enclosed flooded space, available for payloads, or additional buoyancy in the form of syntactic foam.

4.1. Propulsion and actuation

The ALR1500 is fitted with high aspect ratio wings port and starboard to generate hydrodynamic down force to help overcome the vehicles net positive buoyancy, see Fig. 2. At the aft of the vehicle is a propulsion system comprising of a two bladed propeller which is magnetically coupled to the motor and gearbox in a titanium housing.



(a) Autosub Long Range 1500 propulsive performance from ALR-2 trials in Portland Harbour, 2015.



(b) Autosub Long Range 1500 range and endurance for varying payload power.

Fig. 4. Autosub Long Range propulsive performance, range and endurance versus speed.

The ALR1500 shares the propulsion system used in the ALR6000 vehicles. The prime mover is a dry-mounted 24 V, 170 W, Maxon EC 40 brushless DC motor which drives a 600 mm diameter slow-speed fixed pitch propeller through a two-stage 26:1 ratio planetary gearbox and magnetic coupling, designed for long-term reliability over the extended endurance. The motor driver was developed in house at NOC and uses a PIC18F2431 to implement Pulse Width Modulation (PWM) brushless DC motor drive. The PWM setpoint is controlled on a constant input power feedback-loop. The propeller was designed in-house at NOC and based on the well-proven Wagenigen propeller series (Carlton, 2018), with a modified thickness profile to allow the use of 3D-printed materials for rapid-prototyping and development. A significant skew, and rake were also introduced to reduce the chances of entanglement in marine growth or ghost fishing equipment, common in areas of high biodiversity which are often of interest for scientific exploration.

Four control surfaces are present at the aft of the vehicle, just upstream of the propeller, in a cruciform arrangement. These comprise of: two directly coupled stern planes, a single downwards pointing rudder and a fixed top vertical fin which acts as a mount for emergency beacons and flashers. Following robustness issues with the original ALR6000 control plane actuators, the ALR1500 actuators are now

driven by two Volz oil filled actuator units, this is a common technology with the Deep Explorer glider developed by the Bridges H2020 project (Buisson, 2019).

4.2. Onboard energy

The ALR1500 can be fitted with primary or secondary batteries. For long-range applications it is powered by Tadiran SL2780 Lithium Thionyl Chloride primary cells. Each cell weighs 100 g and has a nominal capacity of 68.4 Wh giving a nominal energy density of over 684 Wh/kg. The large internal dry volume and high available mass budget allow ALR1500 to float 2.5 times the installed batteries currently possible on the existing ALR6000 vehicles. When using lithium primary cells this gives a volume limited installed energy of 95 kWhr. For trials and shorter duration deployments the ALR1500 can be fitted with nickel metal hydride or lithium polymer batteries.

4.3. Baseline sensor fit

The baseline sensor fit for science and navigation is provided in Table 1. Further flooded volume is available forward and aft of the main pressure vessel for the fitting of mission specific payloads.

To enable long-range capability, ALR is equipped with small number of low-power sensors. The navigation sensor suite includes a GPS module to obtain GPS fixes when on the surface; a 6-axis PNI TCM XB compass module for determining the vehicle's attitude; a Sea-Bird SBE 52-MP Conductivity, Temperature and Depth (CTD) probe to measure the operating depth; and an ADCP facing downwards to provide bottom-relative or water-relative velocity. For accurately levelling velocity estimates in a local horizontal reference frame, the ADCP module is integrated with tilt sensors (MEMS accelerometers). Given the operating depth and the horizontally levelled AUV velocity, the vehicle is able to perform simple 2-D dead-reckoning to maintain an estimate of its own position.

The nature of the navigation sensors requires in-water calibration to ensure best possible navigation performance. Biases in the MEMS sensors produce compass heading errors that represent the main limiting factors for highly accurate navigation in reciprocal runs with ADCP bottom track. The calibration method used on-board the ALR1500 estimates the bias of the levelled magnetometer data in the X and Y directions. This method gives extremely good results in practice, as the levelled bias estimates have contributions from both accelerometer and magnetometer biases. The compass calibration is executed on launch, as part of ALR's standard operating procedures. Levelled 2-D magnetometer data are collected while the AUV executes a square box with sides of nominally each 250 m in length. It can be shown that levelled magnetometer data in the $X - Y$ plane are expected to give a circular ring of points, with the centre of the ring indicating the bias. The x, y position of the centre of this circle is evaluated by the AUV on-board system, and subsequently subtracted from the real-time magnetometer levelled X and Y data, prior to calculation of the heading. Heading misalignment between the compass and the ADCP is another issue that causes a navigation error which is proportional to the AUV radial distance run from its last GPS position fix. The ALR on-board system can estimate this offset comparing the GPS-fix and the dead-reckoned paths. Best results are obtained when the AUV has simultaneous access to GPS fixes and ADCP bottom track velocity data in shallow waters (< 150 m), on the surface or with a shallow dive.

5. On-board software

The processing for the ALR1500 is built around a dual core 800 Mhz TRITON-TX6DL Module with i.MX6 UltraLite processor running Yocto Linux. The choice of low power ARM processor is driven by the long range aspirations of the AUV. The On-board Control System (OCS) project (Munafò et al., 2019) has developed a unified software architecture for on-board control of various Autosub vehicles. ALR1500 is the first instantiation of this development and represents a transition from a plethora of different legacy vehicle software architectures to a modern distributed architecture based on the Robot Operating System (ROS) (Quigley et al., 2009).

The OCS system is based on a hybrid-hierarchical model as shown in Fig. 5. As proposed in, among others, Teck et al. (2010) and references therein, it adopts a deliberative-reactive architecture that consists of a set of interacting modules organised in three different layers within the control hierarchy:

- The **Supervisory layer** is in charge of making high-level mission decisions, monitoring the vehicle status and communicating with the remote operator. The control at this level is deliberative, i.e. each module produces an output based on its internal states and inputs coming from its sensors.
- The **Mission layer** is responsible for translating the mission goals, represented as higher-level tasks and demands, into commands for the vehicle level.
- The **Vehicle layer** is responsible for performing low-level vehicle control. It interacts reactively with the vehicle's sensors and actuators. For example, at the hardware level, each actuator of

the ALR1500 is controlled in a distributed manner by a dedicated embedded microcontroller. The microcontroller is in turn monitored and commanded by an actuator-specific application in the Vehicle layer of the OCS.

Each level has different responsibilities and defines the responsiveness and interface requirements for the nodes located within it. The responsibilities of each node within the architecture shown in Fig. 5 are briefly described below.

5.1. Supervisory layer

The multi-month deployment (period from launch through to recovery) drives the concept of operations for ALR1500. As such, each deployment will comprise of many individual missions, with each mission sent typically over Iridium SBD and executed sequentially.

The mission executive starts, coordinates, oversees and controls the execution of missions throughout a deployment. It listens to the safety notifications from the OCS Health System (described later) and instigates a contingency behaviour if any abnormality is observed. The mission executive is implemented through Behaviour Trees (Colledanchise and Ögren, 2018), and it is able to receive new mission scripts containing a list of *manoeuvres* (i.e. high-level mission primitives, such as “go to waypoint”, “track follow”, or “loiter at depth”), and forward these sequentially down to the mission layer.

The structure of the Behaviour Tree, and therefore the behaviour of the vehicle, is entirely configurable from an eXtensible Markup Language (XML) file so it can be easily configured for each specific vehicle and deployment without the need to rebuild any code (Sprague et al., 2018). Fig. 6 shows a simplified behaviour tree used to support the mission execution of ALR1500. At each iteration or tick of the tree, variables and conditions are evaluated to determine what part of the tree should be executed, hence determining the specific behaviour of the vehicle.

Throughout mission execution the status of the AUV and the software operating are monitored via the OCS Health Service (OHS) which aggregates information reported by distributed node Low-level Health Monitors, and reports any abnormality to the Mission Executive. Contingency behaviours (Surface, Stop and Abort) can be configured to trigger on receipt of specific abnormality reports. Abnormalities are also transmitted to the remote operator. Three channels are available for communication with ALR1500, WiFi, Acoustic and Iridium SBD. For over-the-horizon operations, the Iridium SBD primary channel provides the link to the C2 piloting toolchain (see Section 6).

5.2. Mission layer

The mission layer includes the Guidance, Navigation and Control (GNC) system of the vehicle. The direct control chain is composed of a three-module hierarchy, namely (from top to bottom, see Fig. 5):

- the **Obstacle Avoidance** system which forces each manoeuvre coming from the supervisory layer to meet desired mission and/or safety constraints based on sensor measurements of the surrounding environment (Fanelli et al., 2020);
- the **Guidance** system, which translates validated mission primitives into body velocity (surge) and orientation (pitch and heading) commands for the controllers;
- the **Controllers** which compute forces and torques to be applied on the vehicle body to achieve the desired velocity and orientation, and allocates these to the available actuators.

Finally, the **Localiser** provides an estimate of the position, the orientation and the velocity of the vehicle, which is used as the feedback of the control loops.

Effectively, the described control architecture allows depth control to be achieved through a cascaded PID control, as is typical with flight-style AUVs (McPhail and Pebody, 1998; Tanakitkorn et al., 2017), whilst heading control is achieved through a simple PID controller linking heading error to rudder demand.

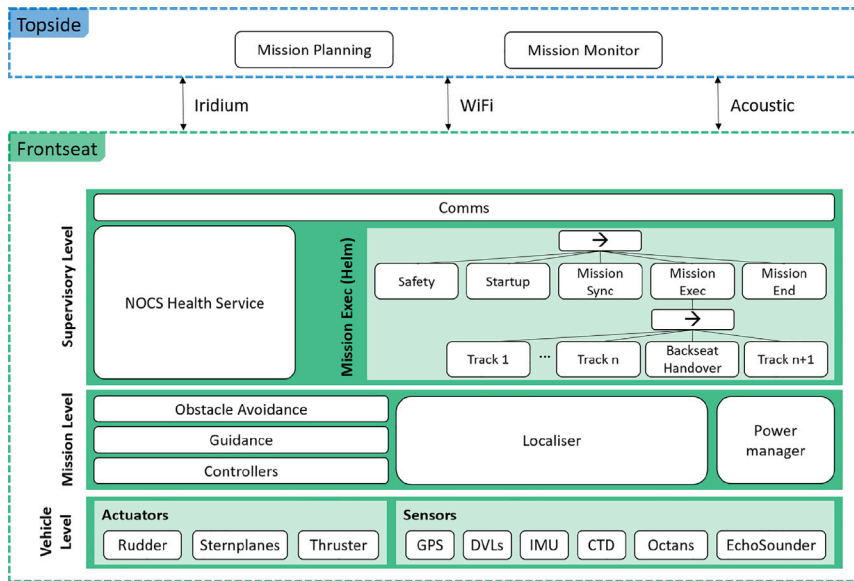


Fig. 5. Simplified control systems basic block diagram.

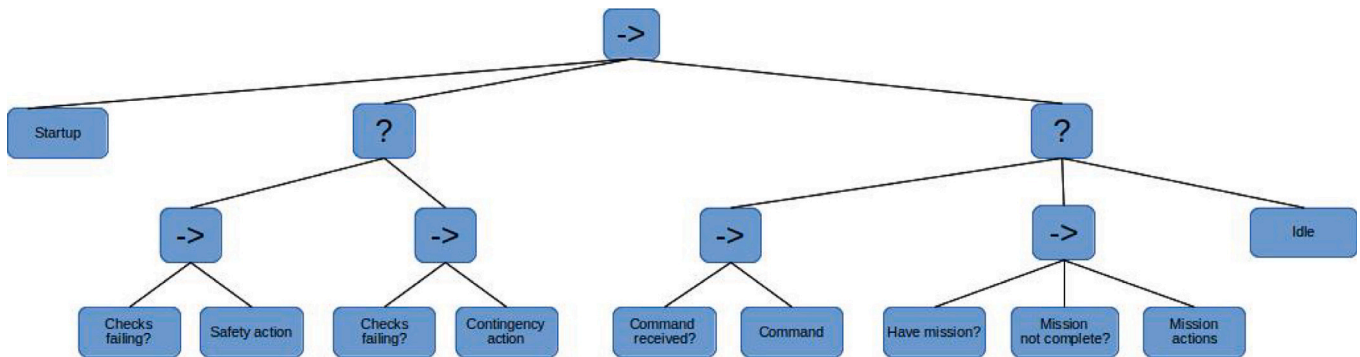


Fig. 6. Schematic of an example ALR1500 Behaviour Tree, defining safety checks, commands and mission execution.

5.3. Vehicle layer

The vehicle layer provides the interface between the mission level and the ALRs equipped devices. This is achieved through a series of driver nodes that manage, the power to devices, the actuator demands and parsing sensor information. All of the sensor and actuator drivers in the vehicle layer implement a health reporting mechanism. This level collects the information and analyses the severity of any device nonconformity. It notifies the OHS node if the severity is high. This system design offers many benefits. It decouples the deliberative part of the system from the low level reactive vehicle control, and hence allows different levels of realtime requirements. Each module has its own private data and implements its own algorithms depending on its assigned responsibilities and goals. All the modules are self-contained and have a uniform software interface to facilitate inter-module communication via the ROS message-passing mechanism.

6. Piloting toolchain

Multi-month operation requires an alternative piloting approach to conventional short range missions. The NOC's C2 project (Harris et al., 2020) is developing a web-based piloting (Farley et al., 2019; Anderlini et al., 2019), monitoring (Anderlini et al., 2021a,b) and data management ecosystem (Hearn et al., 2018) for AUVs, gliders and LRAUVs, which enables multiple vehicles types to be piloted through the same consistent web app. The Oceanids C2 Piloting Framework adopts a

microservice design pattern, a service oriented software architecture in which large applications are built as a suite of smaller, modular, self-contained and loosely-coupled services (Vural et al., 2017). This architecture enables the system to be extended and components to be reconfigured with relative ease for different applications and vehicle integrations, including the ALR1500 class. The C2 provides consistency in the piloting experience between similar vehicle types, so the ALR1500 piloting tools share many design elements with ALR6000 and gliders, reducing the training overhead and likelihood of operator error.

The piloting of LRAUVs necessitates periodic reliable real-time interactions with the vehicles, and sufficient oversight is required to enable remote operators to monitor mission progress despite communication constraints and limited data transfer opportunities. As a result, the core of the C2 architecture is a 'messaging bus' which allows for any microservice, log, user or algorithm to be informed of events across the system as they occur, such as an ALR1500 connecting by satellite to upload data or download a mission. This structure scales especially well to long-duration missions, where it is unlikely that a single human operator will monitor the whole deployment. The messaging bus and microservice architecture enables piloting duties to be seamlessly handed between different users and even automated piloting algorithms, providing consistent information on vehicle and mission state to all stakeholders.

The C2 user interfaces utilises the Material Design framework, designed by Google, which provides a system of guidelines for common User Interface (UI) components and is used throughout Google

products. As a result, many C2 users already have an understanding and familiarity with the look-and-feel of the C2's design and are able to use the system with minimal prior training in comparison to existing piloting tools. As the framework is device agnostic, the interface is suitable for both mobile and desktop web browsers and provides a like-for-like experience.

Normal piloting workflows can be generalised across vehicle types into several key steps: checking the vehicle performance and location, checking the validity of scientific data, making adjustments to the current plan as required, and logging.

6.1. Monitoring vehicle performance

The health page displays the current status of the vehicle including current and previous positions, engineering data and event information detailing previous connection events, aborts etc, see Figs. 7 and 8. The plots are interactive and the user is able to jump all plots through time to a previous point in the mission. For long range missions the C2 can be configured to send notifications to the remote operator when the vehicle surfaces. The C2 can be configured to display third party data products, such as AIS, to aid piloting decision making.

6.2. Scientific data

The contents of the science data page differs depending on the science payload of the particular vehicle on a given deployment. Plots show near real-time data sent from the vehicle mid-mission. Due to communication constraints, this data may be decimated, averaged, sparse etc depending on the vehicle type, but enables remote operator and science users to check the scientific sensors are working as planned and to adjust the sampling or vehicle plan in response to observations made by the vehicle. Near real-time data from NOC operated underwater gliders is automatically sent to the British Oceanographic Data Centre for ingestion, archiving and onward use in data products and forecasting, and it is envisaged that this functionality will be extended to data from ALR1500 in the future.

6.3. Planning tools

The planning tools, shown in Fig. 7, allow the user to construct vehicle-agnostic behaviour-based missions through a visual map-based interface. These plans can be saved for future use and are compiled into vehicle-specific commands which can then be sent immediately to the vehicle via the C2 infrastructure or scheduled for future transfer.

6.4. Pilot log

The C2 allows the remote operator (or pilot) to create log entries from any of the piloting pages. This enables the capture of essential mission metadata, which is then stored alongside the timeseries data from the vehicle itself.

7. Long Distance Proving Trial

Following an extensive series of commissioning trials in Loch Ness, the next stage in the ALR1500 development programme was a demonstration of long-term over-the-horizon operation, thus a Long Distance Proving Trial (LDPT) was defined which would demonstrate the capability of the ALR1500s, in particular for scientific applications. As such, the key objectives of this deployment were:

- Demonstrate the shore launch capability of an ALR1500 coupled with the ability to transit a significant distance to an area of scientific interest;
- Demonstrate various mission capabilities, including a mission to a depth of over 1000 m;

- Demonstrate the capabilities of the NOC C2 system for over-the-horizon piloting of this class of vehicle;
- Prove the operational planning capability of the MARS team. This information and planning process can then be used for future operations;
- Demonstrate a range of sampling strategies.

7.1. Planning

Given the LDPT objectives, an outline deployment plan was constructed in which the ALR1500 would transit from Plymouth out into the Southwest Approaches, travelling out over the shelf break and into the deep sea within the UK Exclusive Economic Zone (EEZ) and back. This route was then refined and subdivided into individual missions separated by a planned surfacing event, to transmit data and receive new instructions. The resulting deployment plan:

1. minimised time spent by the AUV under major shipping routes and, critically, avoided surfacing near shipping lanes or drifting into shipping lanes whilst on the surface;
2. gave sufficient safe margins for navigation drift when operating near shore in regions of high tidal current;
3. avoided key fishing grounds in the English Channel and Southwest Approaches;
4. visited areas of existing scientific interest e.g. South West Deep (West) MPA (JNCC, 2022) and Candyfloss SmartBuoy site (Cefas, 2017);
5. remained within UK EEZ.

The resulting intended route is shown in Fig. 9 in magenta. Key waypoints including surfacing locations are highlighted by diamond symbols (not all waypoints are a surfacing location), as are the extents of the Marine Protected Areas (MPA) discussed above.

7.2. Permissions and notice to mariners

Permissions to operate south of the Plymouth Breakwater were obtained from Queens Harbour Master (Plymouth) and Royal Navy Submarine Command. The Royal Navy, UK Hydrographic Office (UKHO) and Maritime and Coastguard Agency (MCA) were notified of the deployment as were local fishing communities who were notified via the Cornish and Devon Inshore Fisheries and Conservation Authorities (IFCAs) and also the Marine Management Organisation (MMO). The UK MCA Coastal Radio centres and the UKHO were provided with regular updates which were shared as notice to mariners and NAVTEX warnings where appropriate. Due to the comparatively small size of the ALR1500, significantly less than 6 m long, the vehicle was not considered a hazard by UKHO for conventional shipping.

7.3. Risk management

A Hazard Identification (HAZID) was conducted early in the planning cycle and revisited regularly prior to launch to ensure major hazards had been identified and mitigations were proposed and implemented for each stage of the deployment. Broadly, the resulting hazards could be grouped into those associated with: vehicle faults, remote operator errors, and environmental hazards.

7.3.1. Vehicle faults

Hazards associated with the failure of the vehicle were largely mitigated through careful preparation. Established Standard Operating Procedures (SOPs) were followed and a rigorous progression of hardware testing was performed including harbour acceptance tests in Loch Ness, which culminated in a ten day continuous deployment in November/December 2021. This was complemented by a six week software stability test with hardware-in-the-loop to confirm the robustness of the system.

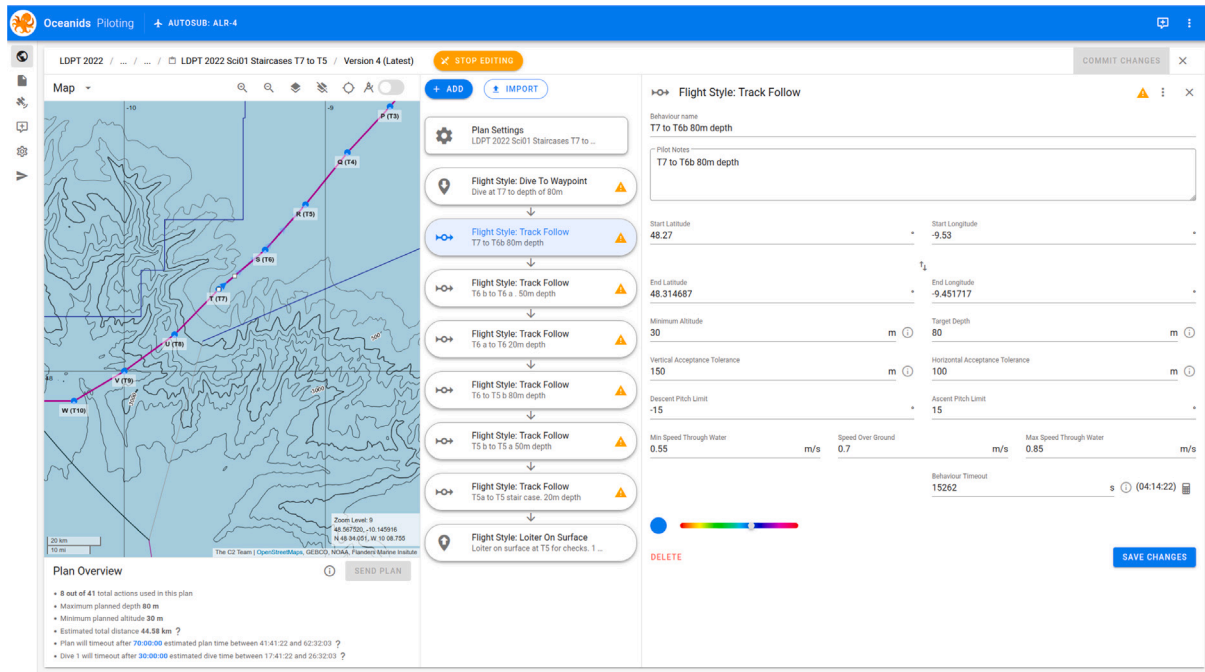


Fig. 7. Example planning cards from the Oceanids C2 web-based piloting tool, illustrating the decimated data received via Iridium SBD.

To mitigate against the need to undertake an unplanned recovery, a selection of potential recovery vessels had been identified which would have been able to recover the AUV whilst in proximity to the coasts of Cornwall and Isles of Scilly. The operating range of these vessels varied from 25 nautical miles (N m) to 60 N m from a point of safe haven. As such, once the AUV was beyond 60 N m from St Mary’s in the Scilly isles, large “Full Ocean” vessels would be the only option for emergency recovery. The deployment was planned to coincide with operations of the NERC vessel *RRS James Cook* which would be operating in the South West Approaches.

7.3.2. Remote operator errors

Hazards associated with remote piloting of the ALR1500s were mitigated through use of the C2 piloting system, coupled with high fidelity simulation of mission plans using a physics based simulator (Manhães et al., 2016) used prior to complex mission plans being sent to the vehicle for execution. The OCS Gazebo Simulator (NGS) is the tool created by NOC to both support testing and debugging of software features, whilst also aiding the anticipation of deployment issues related to physics, mission scripting, software and even hardware. The NGS makes use of the AUV Simulator features to provide a high fidelity Gazebo ROS Simulator which can be interfaced with the entities of the OCS.

The NGS testing helped fix incorrect timeouts set in the mission scripts, confirmed the trajectory of the vehicle for complex missions (e.g. bow-tie and bathtub profiling), and confirm the vehicle configuration. The faster-than-real time simulation lets the operator run a mission four times faster than normal. This means that a 12 h mission would only take 3 h of simulation time. This functionality has been paramount for LDPT deployment containing a large set of long but simple missions. The 43 most complex missions were run in the Simulator prior to deployment.

7.3.3. Environmental hazards

Environmental hazards were largely mitigated through the route planning and the issuing of notice to mariners activities described in Section 7.2.

7.4. Vehicle configuration

For this trial the first in the ALR1500 class of AUVs, ALR-4 was utilised. ALR-4 was equipped with the baseline sensor fit (described in Section 4.3) and augmented with the following additional sensor payload (see Fig. 10).

1. Seabird 43F Dissolved Oxygen (DO) sensor connected directly to the Seabird 52MP CTD sensor,
2. Standalone NOC Lab on Chip Spectrophotometric pH sensor (Yin et al., 2021),
3. Standalone Seabird SeapHOx pH sensor,
4. Wetlabs CDOM Fluorometer (ECO-FLCDRTD)
5. A bespoke long range echo sounder (Huvenne et al., 2019) developed around a 12 kHz Neptune T198 transducer which to provide altitude measurements for ranges between 150 m to 4000 m. Echo sounder readings are intended to form part of a future deep water terrain Aided Navigation System, see Salavasidis et al. (2019, 2021).

7.5. Overview

The route completed is shown in Fig. 9, the black line indicates the dead-reckoned navigation and the red dots indicate GPS position fixes. A breakdown of missions and their key statistics is presented in Table 2. Each significant set of piloting instructions sent to the vehicle is given a mission number, these increment across the life of the AUV, the first 39 missions having been completed in Loch Ness. The estimated distance travelled is calculated based on the distance between waypoints, and does not include the distance travelled to reach the first waypoint, any deviations from the desired trajectory or the distance travelled when loitering at waypoints. Further descriptions of key deployment phases are discussed in the following subsections.

7.6. Launch and calibration missions M40-M44

On the 10th of May 2022, Following final preparations and testing on site in Plymouth, ALR-4 was launched from the Turnchapel

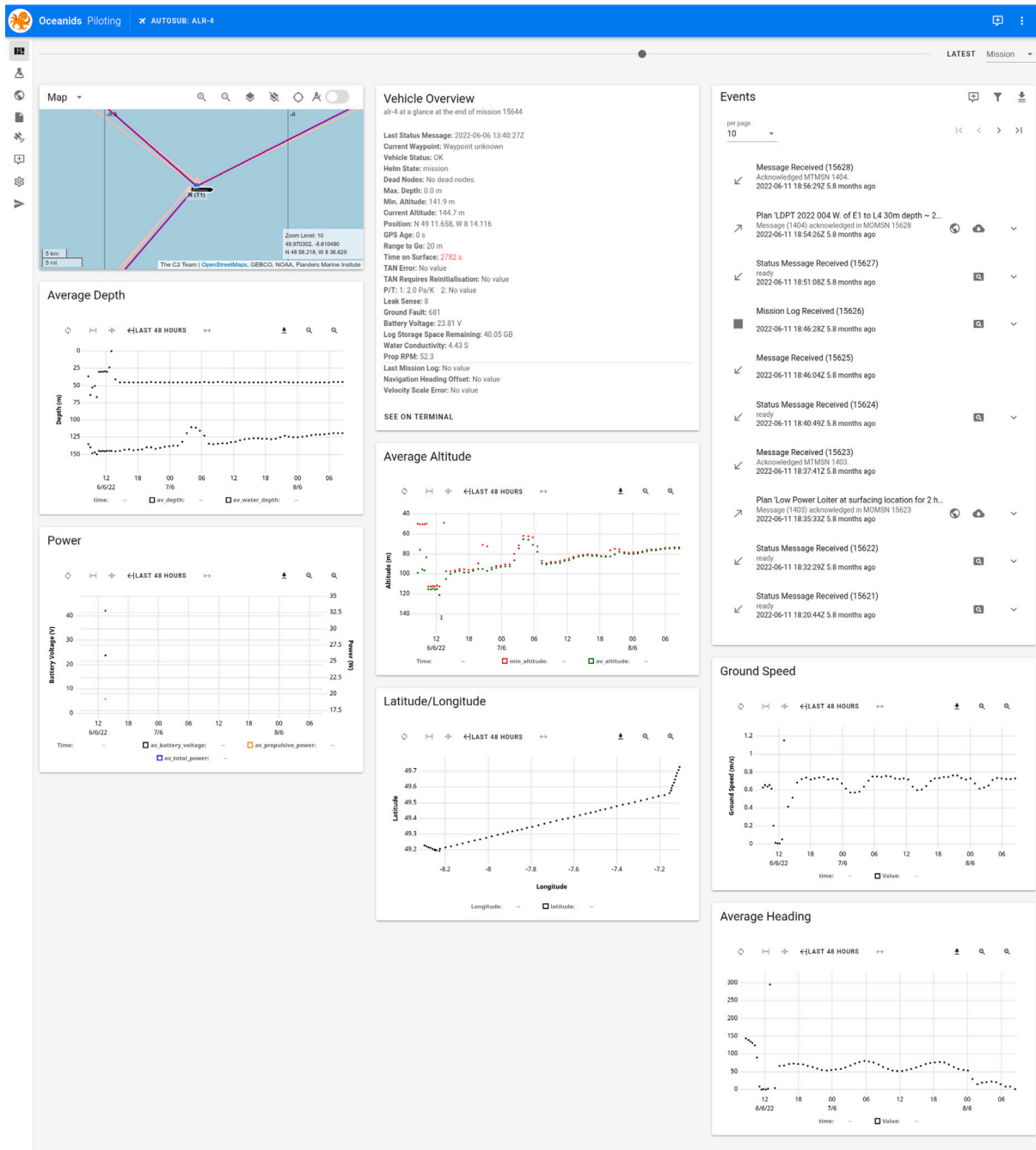


Fig. 8. Example monitoring cards from the C2 piloting tool.

Wharf Marina Crane (see Fig. 11(a)) and towed south of the Plymouth Breakwater by the Thales Rhib *Clyde* with two NOC engineers onboard (see Fig. 11(c)). To minimise risk of damage to the AUV the tow was conducted at slow speed (circa 2 knot), taking approximately 2 h 30 min. The Rhib team rendezvoused with the Plymouth Marine Laboratory research vessel the *PML Quest* south of the Breakwater, where ALR-4 was released from tow, and initial piloting of ALR-4 was undertaken by two other NOC staff onboard the *PML Quest*.

ALR undertook a short series of preparatory missions, consisting of a short run on the surface (M40), a dived box mission to calibrate the compass (M41) and a dived alignment run (M42), prior to transiting underwater to the nominal location of the L4 (Southward et al., 2005) Coastal Station (M43). At the L4 site, piloting was handed over to NOC staff based in Southampton and ALR-4 undertook two steep dives to 40 m (M44) to provide cross calibration with CTD casts from the *PML*

Quest (see Fig. 12) which was acting as a support vessel for the early phases of the deployment.

7.7. Transit from Plymouth to west of the Isles of Scilly M45–M48

At 1615 on the 10th May 2022, ALR-4 was tasked with transiting unaccompanied from L4 to the site of the E1 monitoring station (Smyth et al., 2015) at 30 m altitude (M45) taking a dogleg route to avoid the Eddystone rocks. At 0600 on the 11th May, ALR-4 surfaced within 350 m of the target location at E1 on schedule. M45 had an approximate length of 35 km giving a navigational error of less than 1% of distance travelled. Having safely avoided the first significant hazard to navigation (i.e. Eddystone Rock). ALR-4 continued travelling to the west, heading south of the Lizard and Lands End then travelling to

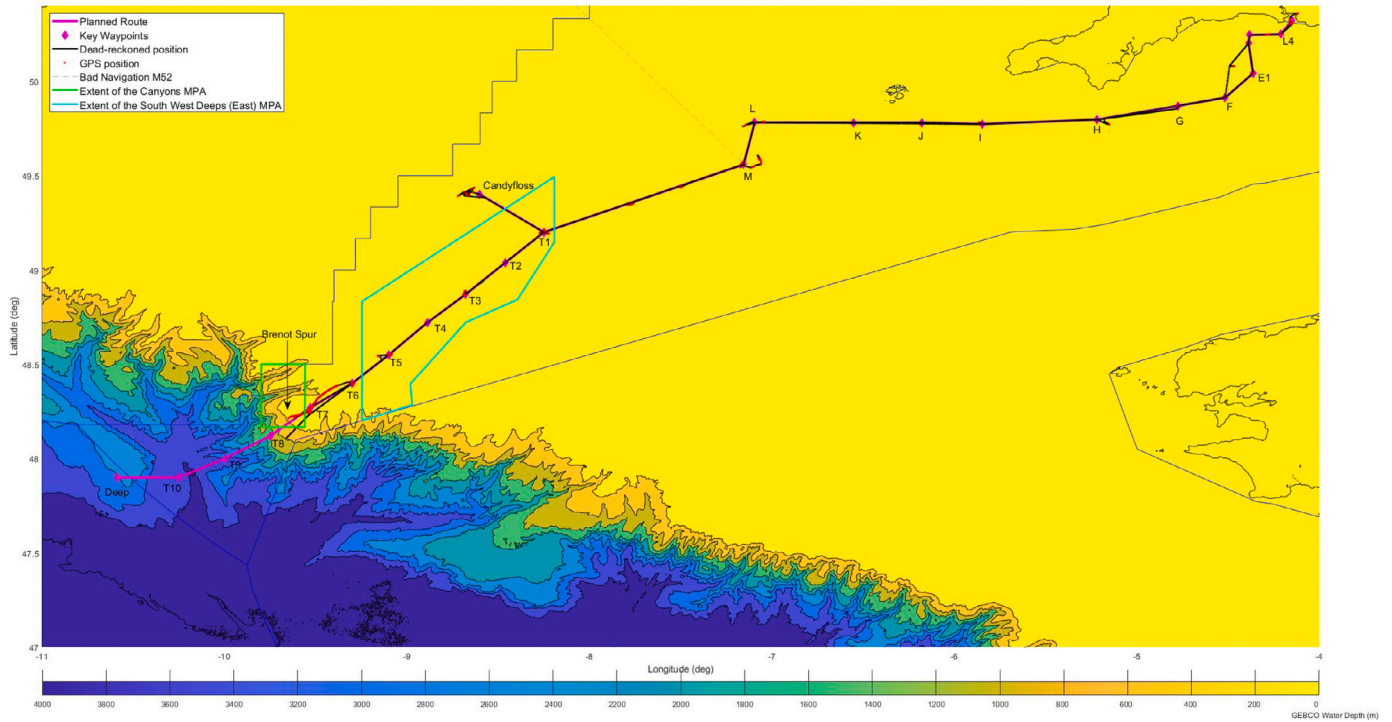


Fig. 9. Planned and completed route, highlighting key waypoints and locations.

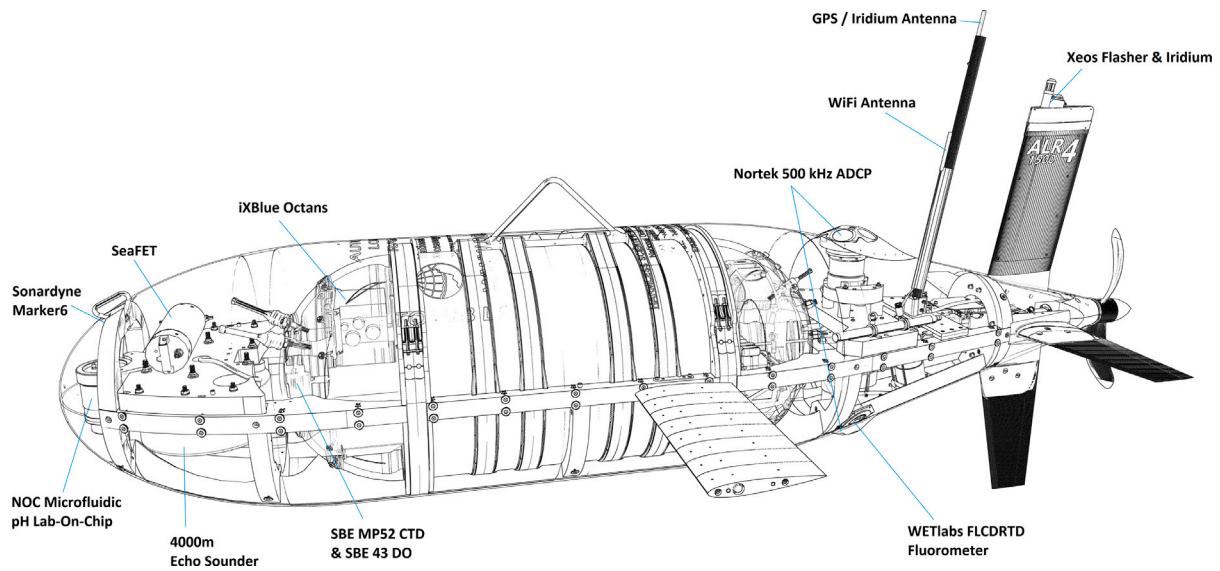


Fig. 10. ALR-4 LDPT configuration.

the south of the Isles of Scilly (M46-48). ALR-4 was surfacing approximately every 12 to 24 h to telemeter data and receive new piloting instructions.

This initial transit enabled the remote operators to learn more about the behaviour of the vehicle when operating near-shore. For these early missions in shallow coastal waters, where ALR-4’s DVL maintained consistent bottom lock (providing the localiser with high quality speed over the ground measurements), the AUV typically surfaced with a navigation error of <2% of distance travelled. However, while operating in this region close to shore, the ALR-4 was observing peak tidal currents

for M48 which varied between of ± 0.35 m/s. As a result, whilst the ALR was able to follow the planned tracks well (<50 m steady state cross track error), large variations in the speed over the ground were observed (the nominal demanded speed through water was 0.7 m/s, whilst the observed speed over the ground varied from 0.35 m/s and 1.05 m/s), and the heading of the vehicle was also affected seeing ± 30 degree variation from the nominal direction to the waypoint. Such high crabbing angles would be detrimental for some potential applications of the ALR1500, particularly photography and swath bathymetry due to the misalignment between sensor swath and direction of travel.

Table 2
Overview of long distance proving trial missions.

Mission number	Mission name	Mission date	Mission time (UTC)	Estimated distance (km)
40	001 Surface Run	10 May 2022	07:11	0.5
41	002 Compass Cal	10 May 2022	07:46	1.2
42	003 Alignment Dive	10 May 2022	10:09	1.4
43	LDPT 2022 001 'Cal' to L4	10 May 2022	11:02	7.4
44	LDPT 2022 001a Profile @L4	10 May 2022	14:32	0
45	LDPT 2022 002 L4 to E1 Check point	10 May 2022	15:15	35
46	LDPT 2022 003 E1 to Int CP 1 (WP E to WP G)	11 May 2022	06:14	37.3
47	LDPT 2022 004 Int CP 1 to Int CP 2	11 May 2022	21:38	77.5
48	LDPT 2022 005 Int CP 2 to WP L	13 May 2022	06:39	90.6
49	LDPT 2022 005a Compass Cal @ wp 'L'	14 May 2022	20:58	1.2
50	LDPT 2022 006b L- >M (CP3) Alignment Dive	14 May 2022	22:41	25.1
51	LDPT 2022 006c Compass Cal @ wp 'M'	15 May 2022	11:00	1.2
52	LDPT 2022 007 Int CP 3 to T1. 30 m depth	15 May 2022	12:50	88.8
53	LDPT 2022 006d Short Dive towards wp 'M'	17 May 2022	20:04	2
54	LDPT 2022 006d Short Dive towards wp 'M'	17 May 2022	21:57	2
55	LDPT 2022 007 Int CP 3 to T1. 60 m Alt 100 m Depth	17 May 2022	23:07	25
56	LDPT 2022 007 Int CP 3 to T1. 60 m Alt 100 m Depth	18 May 2022	12:22	25
57	LDPT 2022 007 Int CP 3 to T1. 60 m Alt 100 m Depth	18 May 2022	23:25	38
58	LDPT 2022 Sci01 Staircases T1 to T3. 50 m Min Alt	19 May 2022	15:15	48
59	LDPT 2022 Sci01 Staircases T3 to T5	20 May 2022	12:39	47
60	LDPT 2022 Sci01 Staircases T5 to T7	21 May 2022	11:52	44.5
61	LDPT 2022 Sci01 Staircases T7 to T9 (50 m altitude)	22 May 2022	07:22	46.2
62	LDPT 2022 Dive towards T7 at 50 m	22 May 2022	12:03	N/A
63	LDPT 2022 Dive towards T7 at 250 m	22 May 2022	12:25	N/A
64	LDPT 2022 Surface run LOS towards T7	22 May 2022	14:19	10.3
65	LDPT 2022 Dive towards T7 at 80 m	22 May 2022	16:41	N/A
66	LDPT 2022 Dive towards T6 at 80 m	23 May 2022	07:10	0.5
67	Emergency Missions - LDPT 2022 Sci01 Const Depth T6 to T5	23 May 2022	10:54	22
68	Loiter at Surface location for 2 h	23 May 2022	21:10	N/A
69	LDPT 2022 Sci01 Staircases T5 to T6	23 May 2022	21:25	22
70	LDPT 2022 Out to 650 m on Brenot Spur	24 May 2022	08:40	73.4
71	LDPT 2022 Out to 1000 m Contour on Brenot Spur	25 May 2022	13:56	85
72	LDPT 2022 Sci01 Staircases T6 to T5	27 May 2022	00:39	22.3
73	Loiter at present location 5 h. Different depths	27 May 2022	11:16	17
74	LDPT 2022 Sci01 Staircases T5 to T3	27 May 2022	17:00	47.1
75	Dive-to-30m_Loiter-Current-Location_1-hours	28 May 2022	14:04	2.5
76	LDPT 2022 Sci01 Staircases T3 to T1	28 May 2022	15:27	48.3
77	Loiter curnt location 5 hr different depths-Hi Spd	29 May 2022	14:17	17
78	Sci07 T1 to CANDYFLOSS Bath tub ±15 Pitch	29 May 2022	20:01	38
79	LDPT 2022 Sci05.3 CANDYFLOSS: Bow Tie WEST	30 May 2022	13:15	48
80	LDPT 2022 Sci05.3 CANDYFLOSS: Bow Tie WEST	31 May 2022	07:29	43.2
81	LDPT 2022 Sci05.3 CANDYFLOSS: Bow Tie WEST 40 m	01 Jun 2022	12:07	43.2
82	Sci08 CF1 Candyfloss Virtual Mooring Profiling WEST	01 Jun 2022	19:05	17
83	LDPT 2022 Sci05.4 CANDYFLOSS: Lawnmower WEST	02 Jun 2022	00:10	43.2
84	Sci09 CF2 Candyfloss V-Mooring Multi Hold Depths W	02 Jun 2022	16:58	47
85	LDPT 2022 Sci05.4 CANDYFLOSS: Lawnmower WEST	03 Jun 2022	18:36	43.2
86	Sci09 CF2 Candyfloss V-Mooring Multi Hold Depths W	04 Jun 2022	11:27	47
87	Sci08 CF1 Candyfloss Virtual Mooring Profile WEST	05 Jun 2022	12:33	17
88	Sci12 West of CANDYFLOSS to T1 Bath tub	05 Jun 2022	15:45	39.4
89	LDPT 2022 001 T1 to WP L. 45 m depth	06 Jun 2022	13:50	113.1
90	LDPT 2022 002 WP L to Lizzard CP. 50 m depth	08 Jun 2022	15:03	134.8
91	LDPT 2022 003 Lizard CP to W. of E1. 50 m depth	10 Jun 2022	14:43	70.7
92	LDPT 2022 004 W. of E1 to L4 30 m depth 25 h	11 Jun 2022	19:00	58.0
93	LDPT 2022 005 standoff to L4	12 Jun 2022	22:00	5.3
94	LDPT 2022 006 L4 to Recovery 2.5 h duration	13 Jun 2022	08:32	7.3

7.8. Failed compass calibration M49–M54

On successfully passing the Isles of Scilly, it was considered advantageous to perform another compass calibration and alignment missions before commencing the science missions, since the expected variation in the Earth's magnetic field declination and horizontal intensity were expected to change by 1 deg and 2% respectively between the initial compass calibration conducted South of the Plymouth Breakwater and Waypoint M. Unfortunately remote operator error and a bug in the OCS resulted in unsuccessful attempts to re-calibrate. M49, the first compass calibration attempted at this location completed earlier than expected and whilst some thought was given to the cause of the early surfacing. The next mission (M50), to move ALR-4 onto the next waypoint, was then run. During this time it was determined that the calibration had failed due to an operator error, in which ALR-4 had not been given

enough time to reach the desired waypoint for the compass calibration to complete successfully. Consequently, a second attempt at a compass calibration (M51) was made at the new location and this appeared to complete successfully. Following the completion of the calibration mission the final long transit mission (M52) was attempted. However, on surfacing from this mission ALR-4 was found to be close to the start waypoint rather than the desired waypoint approximately 90 km south. Suspicion immediately fell on the earlier failed compass calibration, a short test mission confirmed this and as a result the decision was made to reboot the vehicle remotely to return the compass calibration coefficients to those calculated whilst just outside Plymouth. After rebooting, another short test mission was sent to confirm the compass was now behaving as expected and the previously desired long mission was then sent as a series of shorter missions in order to continue to confirm that the navigation was now correct. Post recovery it was determined that there was an underlying software bug in the OCS



(a) Launch from the Turnchapel Wharf Marina Crane



(b) Tow of ALR-4 to south of the Plymouth Breakwater



(c) ALR-4 on station south of the Plymouth Breakwater

Fig. 11. Launch of ALR-4 from Plymouth.

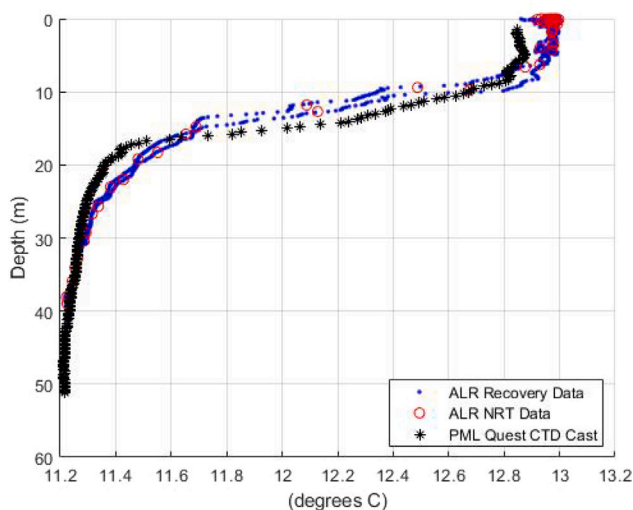


Fig. 12. Temperature Cross Calibration with CTD cast from the *PML Quest* (M44). *PML Quest* CTD data is shown in black. Decimated data provided in near real time to the remote operator via Iridium SBD on completion of the mission is shown in red. Recovery mode data (data recovered from the AUV hardrive on recovery) is shown in blue.

which caused poor calibration values to be applied to the compass in the event of a failed calibration.

7.9. Staircase profiling experiments M58-M60

After transiting to the west of the Isles of Scilly, the focus of the trial switched to the collection of scientific data. Earlier in 2022, an ALR6000 vehicle (ALR-2) equipped with a suite of novel biogeochemical sensors conducted a multi-day deployment from the *RRS Discovery*, travelling the transect T1 to T10 (see Fig. 9) undertaking a staircase profile in the vertical plane with steps at 20 m, 50 m and 80 m depth on the shelf, extending deeper off the shelf. The staircase profiling was adopted to ensure measurements at coincident depths across measurands from independent sensors operating asynchronously with measurement times ranging up to 30 min.

Over the weekend of the 21st/22nd May, the intention had been to repeat this transect from T1 to T10 with ALR-4, running the same staircase profiling. M58 to M60 saw ALR-4 successfully transit towards the shelf break out as far as waypoint T7 (see Fig. 13). M61 should have seen the AUV continue the transect from T7 out to T9 taking the AUV into the deeper water beyond the shelf break. However, at this point the AUV started reporting unrealistic shallow altitudes (distance from the keel of the AUV to the seabed) which forced the AUV to surface (Note in Fig. 13 the noisy and erroneous estimates of water depth starting from approximately 0600 on the 22nd May following the dive at waypoint T7).

Repeated attempts to dive from this location resulted in the AUV returning to the surface as a result of a safety stop condition triggered by the vehicle operating under the minimum specified safe altitude (M62–M63), a safety feature intended to ensure the AUV does not propel itself into the seabed. With the decimated data available over Iridium, it was not entirely clear what was causing the false returns. Further analysis following recovery, indicates the standard device processing of ranges is susceptible to erroneous altitude returns when operating outside of bottom lock, particularly in regions of high productivity or other forms of turbidity, whilst a ten sec persistence is applied to the under safe altitude condition this was being exceeded. This deployment was coincident with the spring bloom and was thus subject to environmental conditions not replicated in other ALR trials. As a post processing exercise additional filtering has been applied to raw range data which has enabled a reduction in false returns. However, it has been deemed necessary to add additional functionality to enable the operator to apply a configurable blanking distance to ignore returns in the top of the water column.

Operation on the surface is one of the higher risk elements of any deployment. Note, at this location near the shelf break the primary concern was wave conditions leading to damage to the AUV actuators leading to lose of vehicle control in the vertical or horizontal plane, shipping in the area was monitored remotely (by AIS) but no vessels were in close proximity (10 km). To get the AUV back underwater, ALR-4 was commanded to transit NE on the surface to the shallow water at waypoint T6. Once there test dives between T6 and T5 and the reciprocal T5 to T6 were completed (M67 and M69) to show the AUV was able to function normally when operating with DVL bottom lock (with the currently fitted Nortek 500 DVLs, reliable bottom lock was observed when operating within 150 m of the bottom).

Having determined the AUV was unable to dive in very deep water the deployment plan was adapted to fly the AUV down the Brenot Spur at a constant altitude, maintaining bottom lock throughout the dive.

7.10. Deep dives following the continental slope M70-M71

In previous trials of the ALR1500 vehicles in Loch Ness, the design was only demonstrated to 220 m depth due to limitations in available water depth. M70 saw the AUV fly down the Brenot Spur to the 650 m contour at a demand altitude Fig. 14

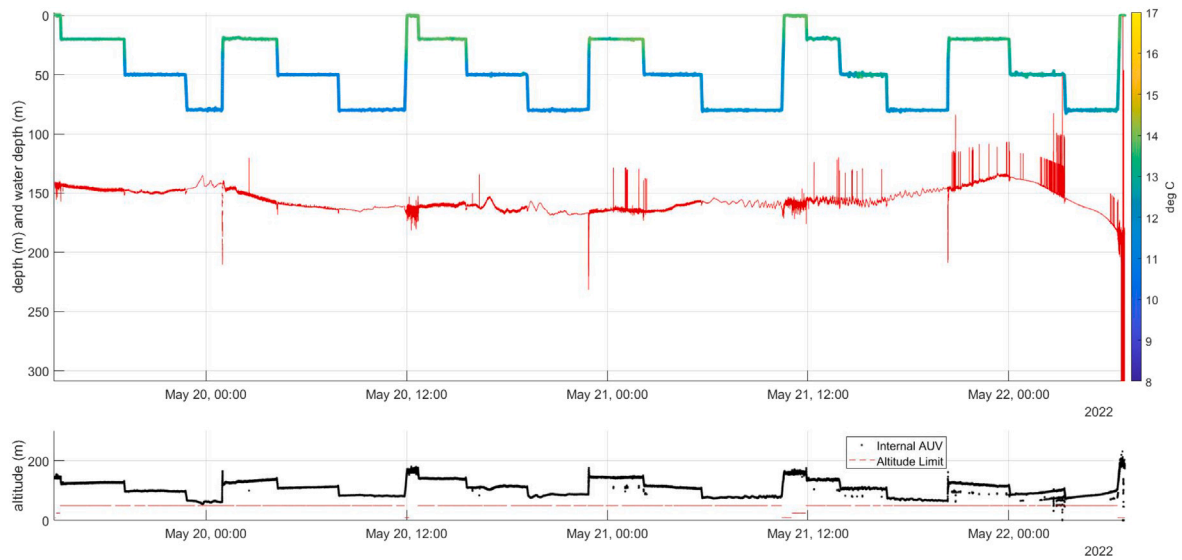


Fig. 13. Staircases from T1 to T7 (M58-60).

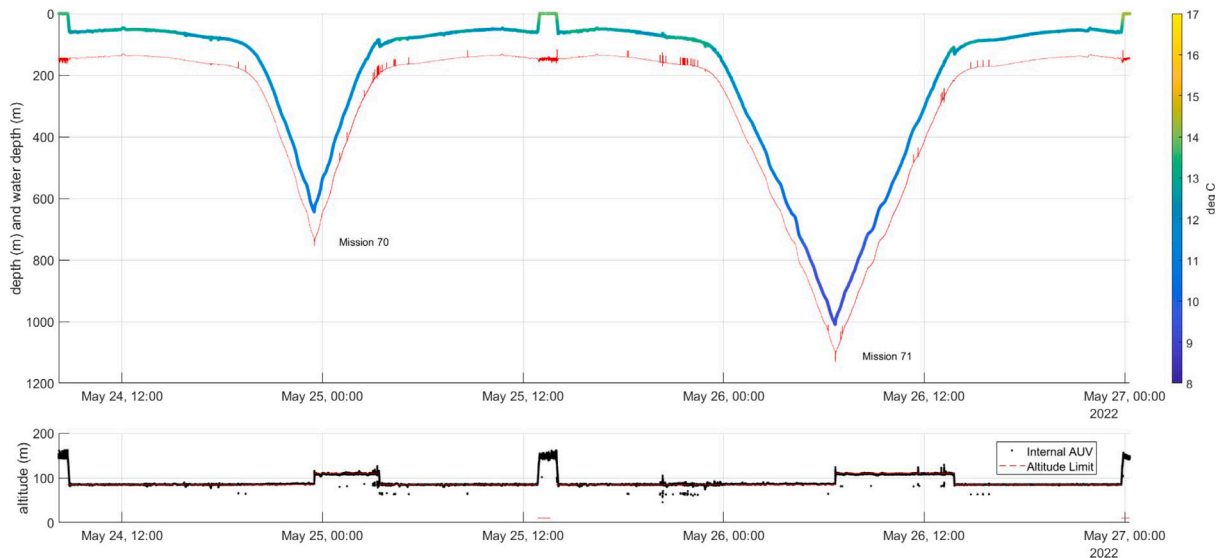


Fig. 14. Vertical Performance M70 and M71. First deep dives of an ALR1500 variant.

- 85 m from T6 to T7a,
- 85 m from T7a to a waypoint on the 650 m contour,
- 110 m from 650 m contour waypoint to T7a,
- 85 m from T7a to T6.

Note the altitude was configured based on the direction and steepness of the slope. For this trial ALR-4 was not fitted with a forward-looking obstacle avoidance system, as such the operator expects the vehicle to overshoot (fly higher than intended altitude) when travelling down the slope, and the vehicle is expected to undershoot (fly closer than intended to the seabed) when travelling up the slope, hence the higher altitude demand on the return from the 650 m contour to T7a.

M71 saw the AUV repeating this activity but flying down to the 1000 m contour. This is the first time NOC have tested the depth rating of a new AUV whilst operating over the horizon, typically this activity would be undertaken with a research vessel in the area, acoustically monitoring the AUV during the dive.

7.11. Bathtub profiling experiments M78 and M88

Whilst ALR-4 is a conventional propeller driven AUV rather than an underwater glider, it is still possible to profile vertically in the water column, an approach favoured by many scientist for capturing vertical gradients (Fossum et al., 2019). Profiling was demonstrated on the transit from T1 to Candyfloss and vice versa (M78 and M88), see Fig. 15. During the descents the node down pitch angle was restricted to -15 deg to ensure ALR-4's downwards pointing DVL was still able to measure altitude and therefore ensure the AUV would not dive into the seabed. For the ascent the pitch angles was limited to 50 degrees resulting in a much faster ascent rate. Note such a high pitch angle means the AUV's DVL is not able to estimate altitude correctly leading to incorrect estimation of water depth (water depth = AUV Depth + Altitude). In the long term the guidance system of the AUV will be upgraded to provide more accurate control on vertical velocity rather than pitch angle. This will enable the AUV to run at very shallow pitch angles providing enhanced vertical resolution.

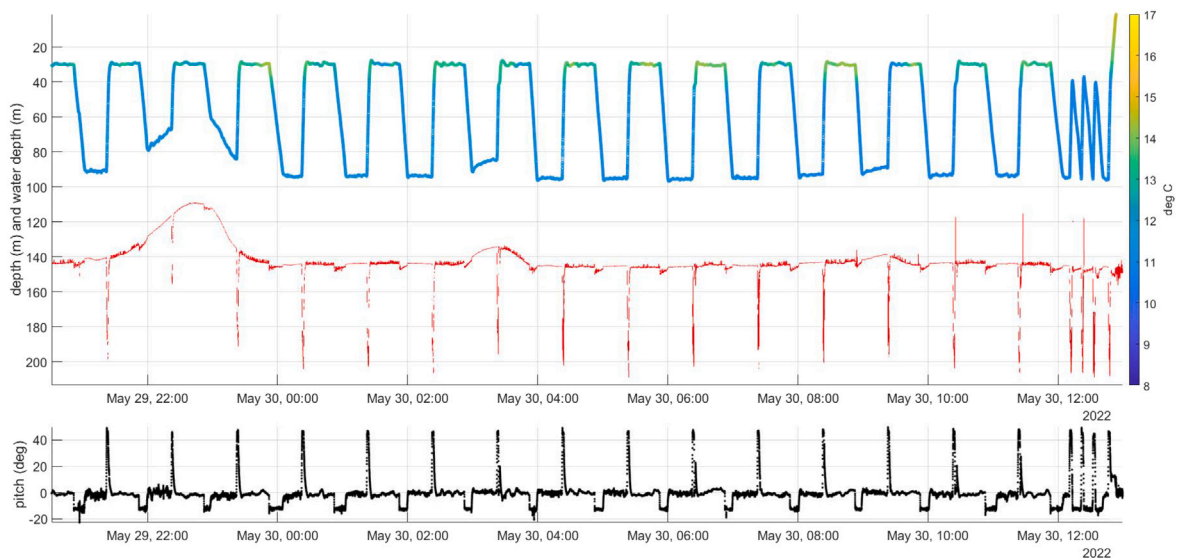


Fig. 15. Sawtooth profiling T1 to Candyfloss (M78).

For an underwater glider the energy use when profiling is concentrated at the bottom of a dive ('Yo') where the glider needs to pump oil into the external bladder to increase the vehicle's buoyancy. Whilst for a propeller driven AUV the energy expenditure is more continuous with some variation between the up and down profiles due to any residual net buoyancy. In practice this is likely to make a propeller driven AUV more efficient than a glider for shallow profiles whereas a glider is more efficient undertaking deep 'Yos' (Rudnick et al., 2004).

7.12. Virtual mooring experiments M79–M87

Whilst most of the LDPT focused on transit style missions the work at the Candyfloss site focused on virtual mooring style missions. Since the AUV is ballasted to be positively buoyant it is not possible with its under-actuated configuration to maintain depth at zero forward speed. Hence, all virtual mooring experiments where conducted at a forward speed. Four survey styles were undertaken. Firstly, 'bow tie' missions over a 1 km² area around the nominal location at a constant depth of 40 m (M81), see Fig. 16(a). Secondly, spiral profiling at a nominal location transitioning from 30 m depth to 30 m altitude (M82), see Fig. 16(b). Thirdly, stacked lawnmower patterns (M85) on a 1 km grid at different depths, see Fig. 16(c). Finally, hold at depth experiments where the AUV loitered at a fixed depth see Fig. 16(d) were ALR-4 loitered at depth for a period of 6 h starting at 30 m altitude then at reducing depths from 120 m, 90 m, 60 m to 30 m deep (M86).

Moorings are a critical component of modern oceanography providing key time series, yet moorings are highly susceptible to being "fished out" by commercial trawlers when deployed on the continental shelf and shelf break, consequently gliders are increasingly being utilised as virtual moorings (Hall et al., 2019). This work demonstrates how moorings could also be complemented by long range AUVs in high risk areas, with the advantage that vehicles such as ALR are able to carry a broader range of sensor payloads than a glider.

Note, some operations in the Candyfloss area were moved 5 km due West due to activities with the *RRS James Cook* (which was also in the area) recovering possible remains of the subsurface element of a Met Office Buoy that had broken free some time ago.

7.13. Recovery

Following 5 weeks of over-the-horizon operation, ALR-4 returned under its own power to the location of the L4 station just south of Plymouth at approximately 09:00 local time, Monday 13th of June, having

travelled approximately 2000 km, spanning 54 missions, including a deep dive to over 1000 m.

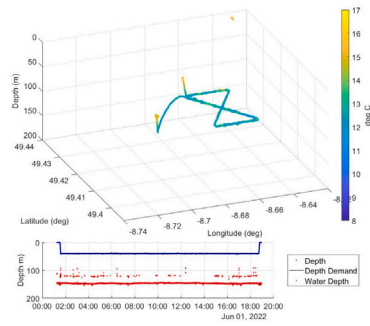
On site to rendezvous was the *PML Quest* undertaking PML's regular weekly sampling. M94 saw the AUV complete two vertical profiles at the L4 station to cross calibrate with the *PML Quest*'s CTD cast, ALR-4 then undertook its final transit of the deployment running at 2 knots from L4 North towards the Plymouth breakwater. Just south of the breakwater the ALR surfaced where it was met by the *RHIB Clyde* from Thales. NOC engineers on board the RHIB placed the AUV on tow and bought it back to Thales' Turnchapel facility. Here the operators were able to extract the complete data set from the AUV control system and sensors.

Inspection of the AUV following the in-water activities highlighted evidence of initial bio-fouling of the AUV. Externally hydroids were seen to be starting to colonise: the propeller hub and growing out from gaps in the hydrodynamic fairings at seam locations (see Fig. 17(a)). Internally, hydroids had started to colonise internal surfaces and actuator lever arms for controlling the rudder and sternplane (see Fig. 17(b)). However, there was no evidence of barnacle growth. There is no significant indication that the minor levels of biofouling were having a measurable impact on hydrodynamic drag and hence power consumption of the vehicle. However, for longer deployments the use of anti-fouling techniques including those discussed in Haldeman et al. (2016), such as seam taping, should be considered. Furthermore, this use of automated detection system to identify changes in hydrodynamic performance attributable to marine growth can be considered, e.g. Anderlini et al. (2021b).

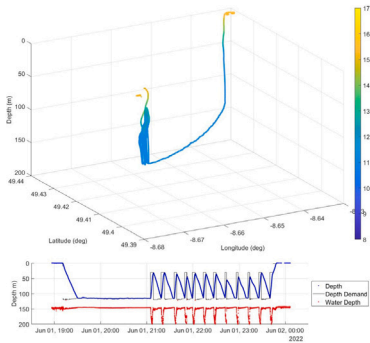
In general, the level of corrosion to metal components was low, the primary anodised aluminium pressure vessel appeared unaffected. There was however, corrosion on an aluminium connector adaptor fitted between a D.G. O'Brien Coax connector for the Iridium/GPS antenna and the main anodised aluminium pressure vessel (see Fig. 17(c)).

8. Conclusions

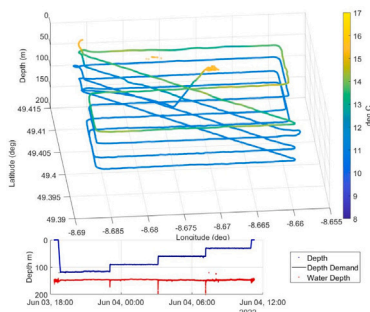
This paper presents the design principals and capabilities of new class of LRAUVs, Autosub Long Range 1500, the latest vehicles to join the Autosub family of AUVs designed and operated by the UK National Oceanography Centre. Unlike conventional AUVs, the ALR1500 has been developed for unaccompanied multi-month operation beyond visual line of sight. This mode of operation presents both new opportunities and challenges for AUV designers, operators, data users and regulators.



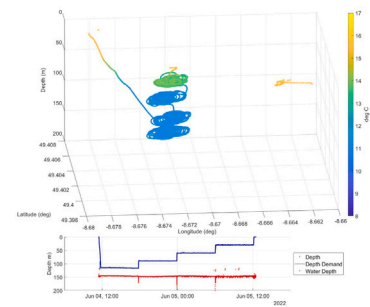
(a) Bow Tie at 40m depth (M81).



(b) Spiral Profiling (M82).



(c) Stacked lawnmower (M85)



(d) Hold At Depth (M86).

Fig. 16. Example virtual mooring strategies.

To demonstrate the capabilities of these new class of vehicle a long distance proving trial was undertaken with the first in class ALR-4. Over a period of five weeks, ALR-4 travelled from Plymouth out to the continental shelf edge south of Ireland and back to Plymouth, covering a distance of almost 2000 km whilst venturing to depths of over 1000 m. Unaccompanied by a support vessel, ALR-4 was instructed



(a) Hydroid growth on hydrodynamic fairing, emanating from the seams between the hydrodynamic fairings.



(b) Hydroid growth on actuator mechanism inside the hydrodynamic fairing.



(c) Corrosion of aluminium connector adaptor between D.G. O'Brien Coax connector for Iridium/GPS antenna and anodised aluminium pressure vessel.

Fig. 17. Example minor defects identified on recovery of ALR-4 in Plymouth.

to surface roughly every 24 h to telemeter sensor data back to operators and receive new piloting instructions from operators based in Southampton. Throughout the deployment the vehicle demonstrated a range of sampling strategies and modes of operations including, level flight transects, profiling, constant altitude terrain following and virtual moorings. Monitoring of the onboard power consumption indicates that approximately half the installed energy was consumed during the trial indicating deployments of three to four months covering 3800 km are realistic with low power payloads.

Whilst extensively tested in inshore waters prior to undertaking this offshore trial, not all elements of the deployment went to plan. Two major new failure modes were identified: a failed compass calibration lead to the AUV being unable to correctly navigate for a period of several days, whilst DVL false returns meant the AUV was unable

to successfully dive directly in deep water. Nether of these failure modes had been captured on previous trials or through desk based activities, highlighting the need for real world testing. Furthermore these trials highlighted limitations in the data being transmitted back to the operator in real time, building on this capability will be a focus moving for future work.

This trial presents a new level of capability for low-carbon technology to meet not just UK, but global marine monitoring requirements. It delivers a highly capable autonomous submarine that can deliver data for scientific research, environmental monitoring, meeting licensing requirements and undertaking industry surveys, at a fraction of the cost of using specialist ships. Such capabilities, open the possibilities of: multi-season time series, vessel free monitoring of decommissioned infrastructure (Jones et al., 2019), shore launch shore recover monitoring of Marine Protected Areas (MPAs), long term monitoring of offshore carbon sequestration sites (Fasham et al., 2015) or complementing routine ocean transects currently undertaken by other types of MAS e.g. gliders on the Ellett Line (Sherwin et al., 2011). Looking further into the future, LRAUVs have the potential to conduct Arctic crossings, a feat currently only possible with large military submarines, (Wadhams et al., 2011), however, this would require significant advances in navigation (Salavasidis et al., 2021).

CRedit authorship contribution statement

Alexander B. Phillips: Writing – original draft, Supervision, Formal analysis. **Robert Templeton:** Methodology. **Daniel Roper:** Methodology. **Richard Morrison:** Methodology. **Miles Pebody:** Software. **Philip M. Bagley:** Supervision. **Rachel Marlow:** Software. **Ed Chaney:** Methodology. **James Burris:** Supervision. **Alberto Consensi:** Software. **Davide Fenucci:** Software. **Francesco Fanelli:** Software. **Achille Martin:** Software. **Georgios Salavasidis:** Software. **Owain Jones:** Software. **Ashley Morris:** Software. **Catherine A. Harris:** Software, Writing – review & editing. **Alvaro Lorenzo:** Software. **Maaten Furlong:** Supervision, Funding acquisition.

Declaration of competing interest

The authors declare that they have no known competing financial interests or personal relationships that could have appeared to influence the work reported in this paper.

Data availability

Data will be made available on request.

Acknowledgements

The development of the ALR1500 was being supported by the Industrial Strategy Challenge Fund/Natural Environment Research Council (NERC) Oceanids Programme and NERC National Underpinning Autonomy Capability funding.

References

Anderlini, E., Harris, C., Phillips, A.B., Lopez, A.L., Woo, M., Thomas, G., 2019. Towards autonomy: A recommender system for the determination of trim and flight parameters for Seagliders. *Ocean Eng.* 189, 106338.

Anderlini, E., Real-Arce, D.A., Morales, T., Barrera, C., Hernandez-Brito, J.J., Phillips, A., Thomas, G., 2021a. A marine growth detection system for underwater gliders. *IEEE Journal of Oceanic Engineering* 46 (4), 1099–1113.

Anderlini, E., Salavasidis, G., Harris, C.A., Wu, P., Lorenzo, A., Phillips, A.B., Thomas, G., 2021b. A remote anomaly detection system for Slocum underwater gliders. *Ocean Engineering* 236, 109531.

Bellingham, J.G., Zhang, Y., Kerwin, J.E., Erikson, J., Hobson, B., Kieft, B., Godin, M., McEwen, R., Hoover, T., Paul, J., et al., 2010. Efficient propulsion for the Tethys long-range autonomous underwater vehicle. In: 2010 IEEE/OES Autonomous Underwater Vehicles. IEEE, pp. 1–7.

Brito, M., Griffiths, G., 2016. A Bayesian approach for predicting risk of autonomous underwater vehicle loss during their missions. *Reliab. Eng. Syst. Saf.* 146, 55–67.

Buisson, N., 2019. BRIDGES project: DXP and UXP gliders bring together research and industry for the development of glider environment services. In: OCEANS 2019-Marseille. IEEE, pp. 1–6.

Carlton, J., 2018. *Marine Propellers and Propulsion*. Butterworth-Heinemann.

Cefas, 2017. Doi: 10.14466/cefadatahub.37. URL: <https://www.cefas.co.uk/data-and-publications/doi/shelf-sea-biogeochemistry-candyfloss-smartbuoy/>.

Chen, X., Bose, N., Brito, M., Khan, F., Thanyamanta, B., Zou, T., 2021. A review of risk analysis research for the operations of autonomous underwater vehicles. *Reliab. Eng. Syst. Saf.* 216, 108011.

Claus, B., Bachmayer, R., 2015. Terrain-aided navigation for an underwater glider. *J. Field Robotics* 32 (7), 935–951.

Colledanchise, M., Ögren, P., 2018. *Behavior Trees in Robotics and AI: An Introduction*. CRC Press.

Connelly, D.P., Copley, J.T., Murton, B.J., Stansfield, K., Tyler, P.A., German, C.R., Van Dover, C.L., Amon, D., Furlong, M., Grindlay, N., et al., 2012. Hydrothermal vent fields and chemosynthetic biota on the world's deepest seafloor spreading centre. *Nature Commun.* 3 (1), 1–9.

Duguid, Z., Camilli, R., 2021. Improving resource management for unattended observation of the marginal ice zone using autonomous underwater gliders. *Front. Robotics AI* 7, 579256.

Fanelli, F., Fenucci, D., Marlow, R., Pebody, M., Phillips, A.B., 2020. Development of a multi-platform obstacle avoidance system for autonomous underwater vehicles. In: 2020 IEEE/OES Autonomous Underwater Vehicles Symposium. AUV, pp. 1–6. <http://dx.doi.org/10.1109/AUV50043.2020.9267942>.

Farley, J., Morris, A.W., Jones, O.D., Harris, C.A., Lorenzo, A., 2019. Marine science from an armchair: A unified piloting framework for autonomous marine vehicles. In: OCEANS 2019-Marseille. IEEE, pp. 1–10.

Fasham, S., Brown, G., Crook, R., 2015. Using acoustics for the monitoring, measurement and verification (MMV) of offshore carbon capture and storage (CCS) sites. In: 2015 IEEE/OES Acoustics in Underwater Geosciences Symposium (RIO Acoustics). pp. 1–9. <http://dx.doi.org/10.1109/RIOAcoustics.2015.7473595>.

Feng, H., Yu, J., Huang, Y., Qiao, J., Wang, Z., Liu, K., 2020. A novel navigation method for autonomous underwater vehicle in the middle water column. In: *Global Oceans 2020: Singapore-US Gulf Coast*. IEEE, pp. 1–6.

Fossum, T.O., Fragoso, G.M., Davies, E.J., Ullgren, J., Mendes, R., Johnsen, G., Ellingsen, I.H., Eidsvik, J., Ludvigsen, M., Rajan, K., 2019. Toward adaptive robotic sampling of phytoplankton in the coastal ocean. *American Association for the Advancement of Science*.

Furlong, M.E., Paxton, D., Stevenson, P., Pebody, M., McPhail, S.D., Perrett, J., 2012. Autosub long range: A long range deep diving AUV for ocean monitoring. In: 2012 IEEE/OES Autonomous Underwater Vehicles (AUV). IEEE, pp. 1–7.

Garabato, A.C.N., Frajka-Williams, E.E., Spingys, C.P., Legg, S., Polzin, K.L., Forryan, A., Abrahamsen, E.P., Buckingham, C.E., Griffies, S.M., McPhail, S.D., et al., 2019. Rapid mixing and exchange of deep-ocean waters in an abyssal boundary current. *Proc. Natl. Acad. Sci.* 201904087.

Garabato, A.C.N., et al., 2017. RRS James Cook cruise JR16005: The dynamics of the orkney passage outflow (DynOPO).

Godin, M., Zhang, Y., Ryan, J., Hoover, T., Bellingham, J., 2011. Phytoplankton bloom patch center localization by the Tethys autonomous underwater vehicle. In: OCEANS'11 MTS/IEEE KONA. IEEE, pp. 1–6.

Graham, A.G., Dutrieux, P., Vaughan, D.G., Nitsche, F.O., Gyllencreutz, R., Greenwood, S.L., Larter, R.D., Jenkins, A., 2013. Seabed corrugations beneath an antarctic ice shelf revealed by autonomous underwater vehicle survey: origin and implications for the history of pine island glacier. *J. Geophys. Res.: Earth Surf.* 118 (3), 1356–1366.

Griffiths, G., 2012. Steps towards autonomy: From current measurements to underwater vehicles. *Methods Oceanogr.* 1, 22–48.

Haldeman, C.D., Aragon, D.K., Miles, T., Glenn, S.M., Ramos, A.G., 2016. Lessening bio-fouling on long-duration AUV flights: Behavior modifications and lessons learned. In: OCEANS 2016 MTS/IEEE Monterey. IEEE, pp. 1–8.

Hall, R.A., Berx, B., Damerell, G.M., 2019. Internal tide energy flux over a ridge measured by a co-located ocean glider and moored acoustic Doppler current profiler. *Ocean Sci.* 15 (6), 1439–1453.

Harris, C., Lorenzo, A., Jones, O., Buck, J., Kokkinaki, A., Loch, S., Gardner, T., Phillips, A.B., 2020. Oceanids C2: An integrated command, control and data infrastructure for the over-the-horizon operation of marine autonomous systems. *Frontiers in Marine Science* 7, 397.

Hayes, D., Boyd, T., Patterson, M., 2007. Sensors and Instrument Requirements for Autonomous Underwater Vehicles. In: *Masterclass in AUV Technology for Polar Science*. SUT, pp. 39–48.

Hearn, M., Kokkinaki, A., Brazier, C., Buck, J., Gardner, T., Jones, O., Loch, S., Lopez, A.L., Philips, A., Thorne, K., et al., 2018. Oceanids command and control (C2) system: Automating marine robot piloting, data transfer and archiving. In: *EGU General Assembly Conference Abstracts*, Vol. 20. p. 14267.

Hobson, B.W., Bellingham, J.G., Kieft, B., McEwen, R., Godin, M., Zhang, Y., 2012. Tethysclass long range AUVs-extending the endurance of propeller-driven cruising AUVs from days to weeks. In: *Autonomous Underwater Vehicles (AUV)*, 2012 IEEE/OES. IEEE, pp. 1–8.

- Huang, Y., Qiao, J., Yu, J., Wang, Z., Xie, Z., Liu, K., 2019a. Sea-whale 2000: A long-range hybrid autonomous underwater vehicle for ocean observation. In: OCEANS 2019 - Marseille. pp. 1–6. <http://dx.doi.org/10.1109/OCEANSE.2019.8867050>.
- Huang, Y., Wang, Z., Yu, J., Zhang, A., Qiao, J., Feng, H., 2019b. Development and experiments of the passive buoyancy balance system for sea-whale 2000 AUV. In: OCEANS 2019 - Marseille. pp. 1–5. <http://dx.doi.org/10.1109/OCEANSE.2019.8867151>.
- Huvenne, V., Furlong, M., et al., 2019. RRS James Cook cruise JC166-167, 19 June–6 July 2018. CLASS–climate-linked atlantic system science Haig Fras marine conservation zone AUV habitat monitoring, equipment trials and staff training.
- Jakuba, M.V., Kaiser, C.L., German, C.R., Soule, A.S., Kelley, S.R., 2018. Toward an autonomous communications relay for deep-water scientific AUV operations. In: 2018 IEEE/OES Autonomous Underwater Vehicle Workshop (AUV). IEEE, pp. 1–7.
- Jenkins, A., Dutrieux, P., Jacobs, S.S., McPhail, S.D., Perrett, J.R., Webb, A.T., White, D., 2010. Observations beneath pine island glacier in west antarctica and implications for its retreat. *Nat. Geosci.* 3 (7), 468–472.
- JNCC, 2022. South West Deeps (east) mpa. URL [https://jncc.gov.uk/our-work/south-west-deeps-east-mpa/#:~:text=South%20West%20Deeps%20\(East\)%20M2C,sea%20bed%20in%20the%20south](https://jncc.gov.uk/our-work/south-west-deeps-east-mpa/#:~:text=South%20West%20Deeps%20(East)%20M2C,sea%20bed%20in%20the%20south).
- Jones, D.O., Gates, A.R., Huvenne, V.A., Phillips, A.B., Bett, B.J., 2019. Autonomous marine environmental monitoring: Application in decommissioned oil fields. *Sci. Total Environ.*
- Kukulya, A.L., Bellingham, J.G., Kaeli, J.W., Reddy, C.M., Godin, M.A., Conmy, R.N., 2016. Development of a propeller driven long range autonomous underwater vehicle (LRAUV) for under-ice mapping of oil spills and environmental hazards: The arctic domain center of awareness project (ADAC). In: 2016 IEEE/OES Autonomous Underwater Vehicles. AUV, pp. 95–100. <http://dx.doi.org/10.1109/AUV.2016.7778655>.
- Manhães, M.M.M., Scherer, S.A., Voss, M., Douat, L.R., Rauschenbach, T., 2016. UUV simulator: A gazebo-based package for underwater intervention and multi-robot simulation. In: OCEANS 2016 MTS/IEEE Monterey. IEEE, pp. 1–8.
- Manley, J.E., Smith, J., 2017. Rapid development and evolution of a micro-UUV. In: OCEANS 2017-Anchorage. IEEE, pp. 1–4.
- MASRWG, 2021. MASS UK Industry Conduct Principles and Code of Practice 2021 (V5).
- McPhail, S., 2009. Autosub6000: A deep diving long range AUV. *J. Bionic Eng.* 6 (1), 55–62.
- McPhail, S.D., Furlong, M.E., Pebody, M., Perrett, J., Stevenson, P., Webb, A., White, D., 2009. Exploring beneath the PIG ice shelf with the Autosub3 AUV. In: Oceans 2009-Europe. IEEE, pp. 1–8.
- McPhail, S.D., Pebody, M., 1998. Navigation and control of an autonomous underwater vehicle using a distributed, networked, control architecture. *Oceanogr. Lit. Rev.* 7 (45), 1240.
- McPhail, S., Templeton, R., Pebody, M., Roper, D., Morrison, R., 2019. Autosub long range AUV missions under the filchner and ronne ice shelves in the weddell sea, antarctica—an engineering perspective. In: OCEANS 2019-Marseille. IEEE, pp. 1–8.
- Medagoda, L., Williams, S.B., Pizarro, O., Kinsey, J.C., Jakuba, M.V., 2016. Mid-water current aided localization for autonomous underwater vehicles. *Auton. Robots* 40 (7), 1207–1227.
- Munafò, A., Pebody, M., Consensi, A., Fanelli, F., Fenucci, D., Fox, P., Marlow, R., Prampart, T., 2019. The NOCS on-board control system. In: OCEANS 2019-Marseille. IEEE, pp. 1–8.
- O'Rourke, R., 2019. Navy Large Unmanned Surface and Undersea Vehicles: Background and Issues for Congress. Congressional Research Service.
- Paull, L., Saeedi, S., Seto, M., Li, H., 2013. AUV navigation and localization: A review. *IEEE J. Ocean. Eng.* 39 (1), 131–149.
- Phillips, A.B., Gold, N., Linton, N., Harris, C.A., Richards, E., Templeton, R., Thuné, S., Sibton, J., Muller, M., Vincent, I., et al., 2017b. Agile design of low-cost autonomous underwater vehicles. In: OCEANS 2017-Aberdeen. IEEE, pp. 1–7.
- Phillips, A., Haroutunian, M., Man, S., Murphy, A., Boyd, S., Blake, J., Griffiths, G., 2012. Nature in engineering for monitoring the oceans: Comparison of the energetic costs of marine animals and AUVs. pp. 373–405. http://dx.doi.org/10.1049/PBCE077E_ch17.
- Phillips, A., Haroutunian, M., Murphy, A.J., Boyd, S., Blake, J., Griffiths, G., 2017a. Understanding the power requirements of autonomous underwater systems, part I: An analytical model for optimum swimming speeds and cost of transport. *Ocean Eng.* 133, 271–279.
- Phillips, A.B., Salavasidis, G., Kingsland, M., Harris, C., Pebody, M., Templeton, D.R.R., McPhail, S., Prampart, T., Wood, T., Taylor, R., et al., 2018. Autonomous surface/subsurface survey system field trials. In: 2018 IEEE/OES Autonomous Underwater Vehicle Workshop (AUV). IEEE, pp. 1–6.
- Qiu, C., Liang, H., Huang, Y., Mao, H., Yu, J., Wang, D., Su, D., 2020. Development of double cyclonic mesoscale eddies at around Xisha islands observed by a 'Sea-Whale 2000' autonomous underwater vehicle. *Appl. Ocean Res.* 101, 102270.
- Quigley, M., Conley, K., Gerkey, B., Faust, J., Foote, T., Leibs, J., Wheeler, R., Ng, A.Y., 2009. ROS: an open-source robot operating system. In: ICRA Workshop on Open Source Software, Vol. 3. Kobe, Japan, p. 5.
- Riser, S.C., Freeland, H.J., Roemmich, D., Wijffels, S., Troisi, A., Belbéoch, M., Gilbert, D., Xu, J., Pouliquen, S., Thresher, A., et al., 2016. Fifteen years of ocean observations with the global argo array. *Nature Clim. Change* 6 (2), 145–153.
- Roper, D., Harris, C.A., Salavasidis, G., Pebody, M., Templeton, R., Prampart, T., Kingsland, M., Morrison, R., Furlong, M., Phillips, A.B., et al., 2021. Autosub long range 6000: a multiple-month endurance AUV for deep-ocean monitoring and survey. *IEEE J. Ocean. Eng.* 46 (4), 1179–1191.
- Roper, D.T., Phillips, A.B., Harris, C.A., Salavasidis, G., Pebody, M., Templeton, R., Amma, S.V.S., Smart, M., McPhail, S., 2017. Autosub long range 1500: An ultra-endurance AUV with 6000 km range. In: OCEANS 2017-Aberdeen. IEEE, pp. 1–5.
- Rudnick, D.L., Davis, R.E., Eriksen, C.C., Fratantoni, D.M., Perry, M.J., 2004. Underwater gliders for ocean research. *Mar. Technol. Soc. J.* 38 (2), 73–84.
- Salavasidis, G., Munafò, A., Fenucci, D., Harris, C.A., Prampart, T., Templeton, R., Smart, M., Roper, D.T., Pebody, M., Abrahamson, E.P., et al., 2020. Terrain-aided navigation for long-range AUVs in dynamic under-mapped environments. *J. Field Robotics.*
- Salavasidis, G., Munafò, A., Harris, C.A., Prampart, T., Templeton, R., Smart, M., Roper, D.T., Pebody, M., McPhail, S.D., Rogers, E., Phillips, A., 2019. Terrain-aided navigation for long-endurance and deep-rated autonomous underwater vehicles. *J. Field Robotics* 36 (2), 447–474.
- Salavasidis, G., Munafò, A., McPhail, S.D., Harris, C.A., Fenucci, D., Pebody, M., Rogers, E., Phillips, A.B., 2021. Terrain-aided navigation with coarse maps—Toward an Arctic crossing with an AUV. *IEEE J. Ocean. Eng.* 46 (4), 1192–1212.
- Sherwin, T.J., Read, J.F., Holliday, N.P., Johnson, C., 2011. The impact of changes in North Atlantic gyre distribution on water mass characteristics in the rockall trough. *ICES J. Mar. Sci.* 69 (5), 751–757.
- Smyth, T., Atkinson, A., Widdicombe, S., Frost, M., Allen, I., Fishwick, J., Queiros, A., Sims, D., Barange, M., 2015. The western channel observatory. *Prog. Oceanogr.* 137 (Part B), 335–341.
- Southward, A.J., Langmead, O., Hardman-Mountford, N.J., Aiken, J., Boalch, G.T., Dando, P.R., Jenner, M.J., Joint, I., Kendall, M.A., Halliday, N.C., et al., 2005. Long-term oceanographic and ecological research in the western english channel. *Adv. Mar. Biol.* 47, 1–105.
- Sprague, C.I., Özkahraman, Ö., Munafò, A., Marlow, R., Phillips, A., Ögren, P., 2018. Improving the modularity of AUV control systems using behaviour trees. In: 2018 IEEE/OES Autonomous Underwater Vehicle Workshop (AUV). IEEE, pp. 1–6.
- Tanakitkorn, K., Wilson, P.A., Turnock, S.R., Phillips, A.B., 2017. Depth control for an over-actuated, hover-capable autonomous underwater vehicle with experimental verification. *Mechatronics* 41, 67–81.
- Teck, T.Y., Chitre, M., Vadakkepat, P., 2010. Hierarchical agent-based command and control system for autonomous underwater vehicles. In: 2010 International Conference on Autonomous and Intelligent Systems, AIS 2010. IEEE, pp. 1–6.
- Testor, P., DeYoung, B., Rudnick, D.L., Glenn, S., Hayes, D., Lee, C., Pattiaratchi, C.B., Hill, K.L., Heslop, E., Turpin, V., et al., 2019. OceanGliders: a component of the integrated GOOS. *Front. Mar. Sci.* 6, 422.
- Underwood, A., Murphy, C., 2017. Design of a micro-AUV for autonomy development and multi-vehicle systems. In: OCEANS 2017-Aberdeen. IEEE, pp. 1–6.
- Veal, R., 2020. Regulation and liability in autonomous shipping: A panoptic view. *Tul. Mar. Law J.* 45, 101.
- Veal, R., Tsimplis, M., Serdy, A., 2019. The legal status and operation of unmanned maritime vehicles. *Ocean Dev. Int. Law* 50 (1), 23–48.
- Vural, H., Koyuncu, M., Guney, S., 2017. A systematic literature review on microservices. In: International Conference on Computational Science and Its Applications. Springer, pp. 203–217.
- Wadhams, P., Hughes, N., Rodrigues, J., 2011. Arctic sea ice thickness characteristics in winter 2004 and 2007 from submarine sonar transects. *J. Geophys. Res.: Oceans* 116 (C8).
- Wynn, R.B., Huvenne, V.A., Le Bas, T.P., Murton, B.J., Connelly, D.P., Bett, B.J., Ruhl, H.A., Morris, K.J., Peakall, J., Parsons, D.R., et al., 2014. Autonomous underwater vehicles (AUVs): Their past, present and future contributions to the advancement of marine geoscience. *Mar. Geol.* 352, 451–468.
- Yang, R., Utne, I.B., Liu, Y., Paltrinieri, N., 2020. Dynamic risk analysis of operation of the autonomous underwater vehicle (AUV). In: Proceedings of the 30th European Safety and Reliability Conference And the 15th Probabilistic Safety Assessment and Management Conference, Italy.
- Yin, T., Papadimitriou, S., Rérolle, V.M., Arundell, M., Cardwell, C.L., Walk, J., Palmer, M.R., Fowell, S.E., Schaap, A., Mowlem, M.C., et al., 2021. A novel lab-on-chip spectrophotometric pH sensor for autonomous in situ seawater measurements to 6000 m depth on stationary and moving observing platforms. *Environ. Sci. Technol.* 55 (21), 14968–14978.
- Zhang, Y., Godin, M.A., Bellingham, J.G., Ryan, J.P., 2012. Using an autonomous underwater vehicle to track a coastal upwelling front. *IEEE J. Oceanic Eng.* 37 (3), 338–347.
- Zhang, X., Wang, C., Jiang, L., An, L., Yang, R., 2021. Collision-avoidance navigation systems for maritime autonomous surface ships: A state of the art survey. *Ocean Eng.* 235, 109380.
- Zhang, Y., Yoder, N., Kiefert, B., Kukulya, A., Hobson, B.W., Ryan, S., Gawarkiewicz, G.G., 2022. Autonomous tracking of salinity-intrusion fronts by a long-range autonomous underwater vehicle. *IEEE J. Oceanic Eng.*